

Aggregation Models with Optimal Weights for Distributed Gaussian Processes

Haoyuan Chen ^a and Rui Tuo ^{a*}

^a Department of Industrial and Systems Engineering
Texas A&M University
College Station, TX 77843, USA

Abstract

GP models have received increasing attention in recent years due to their superb prediction accuracy and modeling flexibility. To address the computational burdens of GP models for large-scale datasets, distributed learning for GPs are often adopted. Current aggregation models for distributed GPs is not time-efficient when incorporating correlations between GP experts. In this work, we propose a novel approach for aggregated prediction in distributed GPs. The technique is suitable for both the exact and sparse variational GPs. The proposed method incorporates correlations among experts, leading to better prediction accuracy with manageable computational requirements. As demonstrated by empirical studies, the proposed approach results in more stable predictions in less time than state-of-the-art consistent aggregation models.

Keywords: Distributed Gaussian processes; Optimized combination technique; Aggregation models; Inducing points.

1 Introduction

Gaussian processes (GPs) (Rasmussen, 2003) are a powerful tool for modeling and inference in various areas of machine learning, such as regression (O’Hagan, 1978; Bishop, 1995), classification (Kuss et al., 2005), signal processing (Liutkus et al., 2011), and robotics and control (Deisenroth et al., 2013). Despite their strengths, GPs face significant challenges when applied to large-scale datasets due to the computational burden of inverting large covariance matrices.

To address these challenges, numerous efficient algorithms have been proposed. Sparse approximations using m inducing points (Titsias, 2009) can reduce the computational complexity from $\mathcal{O}(n^3)$ to $\mathcal{O}(m^2n)$ for a dataset of size n . Wilson and Nickisch (2015) employed structured kernel interpolation combined with Kronecker and Toeplitz algebra to handle a large number of inducing points. Hartikainen and Särkkä (2010) reformulated GP regression as linear-Gaussian state space

*Corresponding author: ruituo@tamu.edu

models, solving them with classical Kalman filtering theory. [Katzfuss and Guinness \(2021\)](#) presented a general Vecchia framework for GP predictions linear computational complexity in the total number of datasets. [Chen et al. \(2022\)](#) represented the kernels via a sparse linear transformation to help reduce complexity. More recently, [Lin et al. \(2023, 2024\)](#) showed that a stochastic dual descent algorithm can efficiently yield competitive GP predictions. However, those approximation methods require at least $\mathcal{O}(n)$ time, which makes them impractical for very large n .

Another direction to address the computational issue is distributed learning, which involves distributing computations across multiple units, often referred to as nodes or experts. In distributed learning ([Dean et al., 2012](#)), the dataset is partitioned and processed in parallel, with results aggregated to form the final model. By applying the previously mentioned GP approximation methods in distributed learning setup across M units, the time complexity can be reduced to $\mathcal{O}(n/M)$. Recent aggregation models for distributed GPs ([Deisenroth and Ng, 2015](#)) rely on independence assumptions and cannot offer *consistent* predictions, meaning the aggregated predictive distribution does not converge to the true underlying predictive distribution as the training size n increases to infinity. To overcome this inconsistency, [Rulli ere et al. \(2018\)](#) introduced the *nested point-wise aggregation of experts* (NPAE), which incorporates covariances between the experts’ predictions but is very time-consuming. [Liu et al. \(2018\)](#) proposed *generalized robust Bayesian committee machine* (grBCM), an efficient and consistent algorithm for distributed GPs.

In this work, we introduce a novel aggregation model for distributed GP to improve time complexity. Our methodology is based on GP regressions using the *optimized combination technique* (OptiCom) introduced in [Section 3](#). The proposed method considers the correlations between the experts to improve the consistency of the aggregated predictions. It is also less time-consuming than NPAE and grBCM when the number of GP experts M is not very large. Empirical studies show that the proposed algorithm outperforms state-of-the-art aggregation models in computational efficiency while providing stable and consistent predictions.

The remainder of this paper is structured as follows: [Section 2](#) reviews the background and related work on GPs and distributed GPs. [Section 3](#) presents the algorithm for extending OptiCom to GP regressions. [Section 4](#) details our proposed algorithm for distributed GPs. [Section 5](#) presents experimental results and comparisons. Finally, [Section 6](#) concludes the paper with discussions.

2 Background

In this section, we provide the necessary background for understanding the proposed methodology. We begin with a review of Gaussian processes in [Section 2.1](#), covering standard GP regression in [Section 2.1.1](#), training procedures in [Section 2.1.2](#), and sparse variational GP approximations in [Section 2.1.3](#). We then introduce distributed GPs in [Section 2.2](#), covering both training strategies in [Section 2.2.1](#) and existing aggregation methods in [Section 2.2.2](#).

2.1 GPs

2.1.1 GP regression

A *Gaussian process* (GP) is a collection of random variables, any finite number of which has a multivariate normal distribution. It is defined by a mean function $\mu(\cdot)$ and a kernel function $k(\cdot, \cdot)$: $f(\cdot) \sim \mathcal{GP}(\mu(\cdot), k(\cdot, \cdot))$.

Suppose we have a set of training points $\mathbf{X} = \{\mathbf{x}_i\}_{i=1}^n$ and the observations $\mathbf{y} = (y_1, \dots, y_n)^\top$ where $y_i = f(\mathbf{x}_i) + \epsilon_i$ with the i.i.d. noise $\epsilon_i \sim \mathcal{N}(0, \sigma_\epsilon^2)$, $f: \mathbb{R}^d \rightarrow \mathbb{R}$ is a latent function. The GP regression imposes a GP prior over the latent function, and we have $\mathbf{f} = f(\mathbf{X}) \sim \mathcal{N}(\boldsymbol{\mu}_f, \mathbf{K}_{ff})$ where $\boldsymbol{\mu}_f = (\mu(\mathbf{x}_1), \dots, \mu(\mathbf{x}_n))^\top$ and $\mathbf{K}_{ff} = [k(\mathbf{x}_i, \mathbf{x}_j)]_{i,j=1}^n$. In this work, we assume f is a zero-mean GP, i.e., $\mu(\cdot) = 0$, the posterior distribution $p(f|\mathbf{y}) = \mathcal{N}(\mu_{f|\mathbf{y}}, k_{f|\mathbf{y}})$ takes the form

$$\mu_{f|\mathbf{y}}(\cdot) = \mathbf{K}_{(\cdot)f} \tilde{\mathbf{K}}_{ff}^{-1} \mathbf{y}, \quad (1a)$$

$$k_{f|\mathbf{y}}(\cdot, \cdot') = k(\cdot, \cdot') - \mathbf{K}_{(\cdot)f} \tilde{\mathbf{K}}_{ff}^{-1} \mathbf{K}_{f(\cdot')}, \quad (1b)$$

where $\tilde{\mathbf{K}}_{ff} = \mathbf{K}_{ff} + \sigma_\epsilon^2 \mathbf{I}_n$ is the covariance matrix of all training points \mathbf{X} with diagonal observation noise, $\sigma_\epsilon^2 > 0$ is the noise variance, \mathbf{I}_n is a $n \times n$ identity matrix, $\mathbf{K}_{(\cdot)f} = k(\cdot, \mathbf{X}) = [k(\cdot, \mathbf{x}_i)]_{i=1}^n = k(\mathbf{X}, \cdot)^\top = \mathbf{K}_{f(\cdot)}^\top$ is the cross-covariance matrix.

2.1.2 GP training

The hyperparameters $\boldsymbol{\theta}$ of GPs, which may include GP variance, kernel lengthscale, are commonly learned by maximizing the *log-marginal likelihood* $\mathcal{L}(\boldsymbol{\theta}) = \log p(\mathbf{y}|\mathbf{f}; \boldsymbol{\theta})$. A standard way of obtaining the optimized hyperparameters is by taking the derivative of each $\theta \in \boldsymbol{\theta}$.

2.1.3 Sparse variational GP (SVGP)

Exact GP regression and training as described in [Section 2.1.1](#) and [Section 2.1.2](#) require $\mathcal{O}(n^3)$ time due to the computation of the terms $\tilde{\mathbf{K}}_{\mathbf{ff}}^{-1}$, $\log \det(\tilde{\mathbf{K}}_{\mathbf{ff}}^{-1})$, and $\text{tr}\left(\tilde{\mathbf{K}}_{\mathbf{ff}}^{-1} \frac{\partial \tilde{\mathbf{K}}_{\mathbf{ff}}}{\partial \theta}\right)$, which is prohibitive when n is large. To solve this problem, [Titsias \(2009\)](#) introduced *sparse variational Gaussian process* (SVGP), a variational framework for sparse GPs using $m \ll n$ inducing variables $\mathbf{u} = (u_1, \dots, u_m)^\top$ with m associated inducing inputs $\mathbf{Z} = \{\mathbf{z}_i\}_{i=1}^m$, $\mathbf{z}_i \in \mathbb{R}^d$, which reduces the time complexity to $\mathcal{O}(nm^2)$. The variational distribution $q(\mathbf{u}) = \mathcal{N}(\mathbf{m}_{\mathbf{u}}, \mathbf{S}_{\mathbf{uu}})$ yields the predictive distribution $\hat{q}(f) = \mathcal{N}(\hat{\mu}_f^{\mathbf{u}}, \hat{k}_f^{\mathbf{u}})$ as follows:

$$\hat{\mu}_f^{\mathbf{u}}(\cdot) = \sigma_\epsilon^{-2} \mathbf{K}_{(\cdot)\mathbf{u}} \mathbf{M}_{\mathbf{uu}}^{-1} \mathbf{K}_{\mathbf{uf}} \mathbf{y}, \quad (2a)$$

$$\hat{k}_f^{\mathbf{u}}(\cdot, \cdot') = k(\cdot, \cdot') - \mathbf{K}_{(\cdot)\mathbf{u}} (\mathbf{K}_{\mathbf{uu}}^{-1} - \mathbf{M}_{\mathbf{uu}}^{-1}) \mathbf{K}_{\mathbf{u}(\cdot')}, \quad (2b)$$

where $\mathbf{K}_{(\cdot)\mathbf{u}} = [k(\cdot, \mathbf{z}_i)]_{i=1}^m = \mathbf{K}_{\mathbf{u}(\cdot)}^\top$, $\mathbf{K}_{\mathbf{uf}} = [k(\mathbf{z}_i, \mathbf{x}_j)]_{i,j=1}^{m,n} = \mathbf{K}_{\mathbf{fu}}^\top$, and $\mathbf{M}_{\mathbf{uu}} = [\mathbf{K}_{\mathbf{uu}} + \sigma_\epsilon^{-2} \mathbf{K}_{\mathbf{uf}} \mathbf{K}_{\mathbf{fu}}]$.

The SVGP framework introduced here is essential for our distributed learning methodology in [Section 4](#). By employing SVGP approximations at the local expert level before aggregation, we achieve a double reduction in computational cost: first, inducing points approximation reduces the cost from $\mathcal{O}(n^3)$ to $\mathcal{O}(nm^2)$; second, data parallelization across M experts further reduces the time complexity to $\mathcal{O}(nm^2/M)$.

2.2 Distributed GP

While SVGP reduces complexity from $\mathcal{O}(n^3)$ to $\mathcal{O}(nm^2)$, this can still be impractical when n is extremely large such as billions of observations. Distributed learning provides a natural solution by partitioning the data across M computational units (experts) and processing them in parallel, further reducing per-unit complexity to $\mathcal{O}(nm^2/M)$.

This section introduces the distributed GP framework that motivates our main contributions. [Section 2.2.1](#) describes how local experts are trained independently on partitioned local datasets. [Section 2.2.2](#) reviews existing aggregation methods for distributed GPs and highlights their strengths and limitations.

2.2.1 Distributed GP training

Distributed GPs ([Deisenroth and Ng, 2015](#)) enable the parallel training of GPs across different experts to accelerate the computing process for large-scale datasets. Note that distributed GPs are

not inherently private because they involve data sharing or centralized aggregation, whereas federated GPs preserve privacy by keeping raw data local and only exchanging model updates. Assuming the same model as in [Section 2.1.1](#), we first partition the global training dataset $\mathcal{D} := \{\mathbf{X}, \mathbf{y}\}$ of size n into M local datasets $\mathcal{D}_i = \{\mathbf{X}_i, \mathbf{y}_i\}$, each of size n_i for $i = 1, \dots, M$. Each local dataset \mathcal{D}_i corresponds to an expert \mathcal{M}_i . Clearly, $n = \sum_{i=1}^M n_i$. We suppose that all local datasets share the same hyperparameters $\boldsymbol{\theta}$. The global objective for distributed GP training is to maximize the global marginal log-likelihood $\log p(\mathbf{y}|\mathbf{f}, \boldsymbol{\theta})$, where $\mathbf{f} = f(\mathbf{X})$. Assuming independence among all the experts $\{\mathcal{M}_i\}_{i=1}^M$, the global marginal log-likelihood is approximated as:

$$\log p(\mathbf{y}|\mathbf{f}; \boldsymbol{\theta}) \approx \sum_{i=1}^M \log p_i(\mathbf{y}_i|\mathbf{f}_i; \boldsymbol{\theta}) = -\frac{1}{2} \sum_{i=1}^M \left(\mathbf{y}_i^\top \tilde{\mathbf{K}}_{\mathbf{f}_i \mathbf{f}_i}^{-1} \mathbf{y}_i + \log \det(\tilde{\mathbf{K}}_{\mathbf{f}_i \mathbf{f}_i}) + n_i \log(2\pi) \right) \quad (3)$$

where $p_i(\mathbf{y}_i|\mathbf{f}_i; \boldsymbol{\theta}) \sim \mathcal{N}(\mathbf{0}, \tilde{\mathbf{K}}_{\mathbf{f}_i \mathbf{f}_i})$ is the local marginal likelihood of the i -th model \mathcal{M}_i with $\tilde{\mathbf{K}}_{\mathbf{f}_i \mathbf{f}_i} = \mathbf{K}_{\mathbf{f}_i \mathbf{f}_i} + \sigma_\epsilon^2 \mathbf{I}_{n_i}$ and $\mathbf{K}_{\mathbf{f}_i \mathbf{f}_i} = k(\mathbf{X}_i, \mathbf{X}_i) \in \mathbb{R}^{n_i \times n_i}$, $\mathbf{f}_i = f(\mathbf{X}_i) \in \mathbb{R}^{n_i}$.

The factorized approximation of the log-likelihood in [eq. \(3\)](#) (FACT) approximates the full covariance matrix $\mathbf{K}_{\mathbf{ff}} = k(\mathbf{X}, \mathbf{X})$ by a diagonal block matrix $\text{diag}[\mathbf{K}_{\mathbf{f}_1 \mathbf{f}_1}, \dots, \mathbf{K}_{\mathbf{f}_M \mathbf{f}_M}]$, reducing the time complexity to $\mathcal{O}(n^3)$. Other optimization techniques include Federated Averaging (FedAvg) ([McMahan et al., 2017](#)), which averages local model updates; FedProx ([Li et al., 2020](#)), which improves FedAvg by addressing client heterogeneity; ADMM ([Boyd et al., 2011](#)), which solves a consensus optimization problem by introducing auxiliary variables and dual updates.

2.2.2 Aggregated prediction

After training local experts, we aggregate local predictions to form a global prediction. Let $\mu_i(\cdot)$ and $\sigma_i^2(\cdot)$ denote the predictive mean and variance from expert \mathcal{M}_i . Common aggregation methods for GP experts include *product-of-experts* (PoE) ([Hinton, 2002](#)), *generalised product-of-experts* (gPoE) ([Cao and Fleet, 2014](#)), *Bayesian committee machine* (BCM) ([Tresp, 2000](#)), *robust Bayesian committee machine* (rBCM) ([Deisenroth and Ng, 2015](#)), *generalized robust Bayesian committee machine* (grBCM) ([Liu et al., 2018](#)), and *nested pointwise aggregation of experts* (NPAE) ([Rullière et al., 2018](#)). PoE, gPoE, BCM and rBCM produce a global prediction using a weighted average of local precisions, the joint mean $\mu_{\mathcal{A}}$ and joint precision $\sigma_{\mathcal{A}}^{-2}$ are given by

$$\mu_{\mathcal{A}}(\cdot) = \sigma_{\mathcal{A}}^2(\cdot) \sum_{i=1}^M \beta_i \sigma_i^{-2}(\cdot) \mu_i(\cdot), \quad (4a)$$

$$\sigma_{\mathcal{A}}^{-2}(\cdot) = \sum_{i=1}^M \beta_i \sigma_i^{-2}(\cdot) + \left(1 - \sum_{i=1}^M \beta_i\right) \sigma_{**}^{-2}(\cdot), \quad (4b)$$

where $\sigma_{**}^{-2}(\cdot) = k(\cdot, \cdot) + \sigma_\epsilon^2$ is the prior variance, serving as a correction term for the BCM family. The weights, β_i , are defined as follows: $\beta_i = 1$ for PoE and BCM, and $\beta_i = 0.5(\log \sigma_{**}^2(\cdot) - \log \sigma_i^2(\cdot))$ for gPoE and rBCM.

For grBCM, the M experts are divided into two groups: the global expert \mathcal{M}_c , trained on dataset $\mathcal{D}_c = \mathcal{D}_1$ of size n_c , and the local experts $\{\mathcal{M}_i\}_{i=2}^M$, trained on datasets $\{\mathcal{D}_i\}_{i=2}^M$. The augmented dataset $\mathcal{D}_{+i} = \{\mathcal{D}_c, \mathcal{D}_i\}$ leads to a new expert \mathcal{M}_{+i} for $i = 2, \dots, M$. The joint mean and joint precision are given by:

$$\mu_{\mathcal{A}}(\cdot) = \sigma_{\mathcal{A}}^2(\cdot) \left(\sum_{i=2}^M \beta_i \sigma_{+i}^{-2}(\cdot) \mu_{+i}(\cdot) - \left(\sum_{i=2}^M \beta_i - 1 \right) \sigma_c^{-2}(\cdot) \mu_c(\cdot) \right), \quad (5a)$$

$$\sigma_{\mathcal{A}}^{-2}(\cdot) = \sum_{i=2}^M \beta_i \sigma_{+i}^{-2}(\cdot) - \left(\sum_{i=2}^M \beta_i - 1 \right) \sigma_c^{-2}(\cdot), \quad (5b)$$

where μ_c and σ_c^{-2} are the mean and precision of expert \mathcal{M}_c , and μ_{+i} and σ_{+i}^{-2} are the mean and precision of expert \mathcal{M}_{+i} . The weights are defined as $\beta_2 = 1$, and $\beta_i = 0.5(\log \sigma_c^2(\cdot) - \log \sigma_{+i}^2(\cdot))$ for $i = 3, \dots, M$.

NPAE leverages the covariances between experts to ensure consistent predictions. The joint mean and joint variance are computed as follows:

$$\mu_{\mathcal{A}}(\cdot) = \mathbf{K}_{(\cdot)\mathcal{A}} \mathbf{K}_{\mathcal{A}\mathcal{A}}^{-1} \boldsymbol{\mu}_{\mathcal{A}}, \quad (6a)$$

$$\sigma_{\mathcal{A}}^2(\cdot) = k(\cdot, \cdot) - \mathbf{K}_{(\cdot)\mathcal{A}} \mathbf{K}_{\mathcal{A}\mathcal{A}}^{-1} \mathbf{K}_{\mathcal{A}(\cdot)} + \sigma_\epsilon^2, \quad (6b)$$

where $\mathbf{K}_{(\cdot)\mathbf{f}_i} = k(\cdot, \mathbf{X}_i) = \mathbf{K}_{\mathbf{f}_i(\cdot)}^\top$, $\mathbf{K}_{\mathbf{f}_i\mathbf{f}_j} = k(\mathbf{X}_i, \mathbf{X}_j)$, $\tilde{\mathbf{K}}_{\mathbf{f}_i\mathbf{f}_i} = \mathbf{K}_{\mathbf{f}_i\mathbf{f}_i} + \sigma_\epsilon^2 \mathbf{I}_{n_i}$. $\mathbf{K}_{\mathcal{A}(\cdot)} = [\text{cov}[\mu_i(\cdot), y_*(\cdot)]]_{i=1}^M$
 $= \mathbf{K}_{(\cdot)\mathcal{A}}^\top \in \mathbb{R}^M$, $\mathbf{K}_{\mathcal{A}\mathcal{A}} = [\text{cov}[\mu_i(\cdot), \mu_j(\cdot)]]_{i,j=1}^M \in \mathbb{R}^{M \times M}$, $\boldsymbol{\mu}_{\mathcal{A}} = [\mu_1(\cdot), \dots, \mu_M(\cdot)]^\top \in \mathbb{R}^M$.

Among these methods, PoE, gPoE, BCM, and rBCM are computationally efficient but assume independence between experts, leading to inconsistent predictions as the dataset size grows. The grBCM method addresses consistency by introducing a global expert but requires training augmented models \mathcal{M}_i^+ for $i = 2, \dots, M$, each on datasets of size $n_c + n_i$, significantly increasing computational cost. NPAE accounts for correlations through the full covariance matrix $\mathbf{K}_{\mathcal{A}\mathcal{A}}$ in eq. (6), achieving consistency but at $O(M^3)$ cost for inverting this matrix, which becomes prohibitive for large M .

These limitations motivate our approach: we seek an aggregation method that (1) incorporates expert correlations for consistency, (2) maintains computational efficiency comparable to simple baselines, and (3) naturally applies to both exact GP and SVGP settings. Our key insight introduced in [Section 4](#) is to leverage the optimized combination technique (OptiCom) from sparse grid theory, which is introduced in [Section 3](#), to derive optimal aggregation weights that address these requirements.

3 GP regression with OptiCom

This section introduces GP regression using the optimized combination technique (OptiCom). We first review the standard combination technique (CT) in [Section 3.1](#), followed by OptiCom in [Section 3.2](#), and then show how it is applied to GP regression.

3.1 Combination technique (CT)

Combination technique (CT) ([Griebel et al., 1990](#); [Hegland et al., 2007](#)), first introduced in ([Smolyak, 1963](#)), is an efficient tool for approximating the sparse grid spaces. When partial projection operators commute, as in interpolation with tensor product spaces, the combination technique provides the exact sparse grid solution. Sparse grids of level η and dimension d are defined as ([Garcke, 2013](#))

$$\Omega_\eta^d := \bigcup_{|\underline{l}|_1 = \eta + d - 1} \Omega_{\underline{l}} = \bigcup_{|\underline{l}|_1 = \eta + d - 1} \Omega_{l_1}^1 \times \cdots \times \Omega_{l_d}^1. \quad (7)$$

Here, $\underline{l} = (l_1, \dots, l_d)$, $|\underline{l}|_1 = \sum_{j=1}^d l_j$, where $l_j \in \mathbb{N}^+$ for all $j = 1, \dots, d$. $\Omega_{l_1}^1 \times \cdots \times \Omega_{l_d}^1 = \{(\omega_{l_1}, \dots, \omega_{l_d}) | \omega_{l_j} \in \Omega_{l_j}^1 \text{ for } j \in \{1, \dots, d\}\}$ denotes the n -ary Cartesian product over d one-dimensional set $\Omega_{l_j}^1 \subset \mathbb{R}$, $j = 1, \dots, d$. We suppose $\Omega_{l_j}^1$ consists of 2^{l_j-1} uniformly distributed points over a fixed interval, i.e., $\Omega_{l_j}^1$ over the interval $[0, 1]$ is given by $\Omega_{l_j}^1 = \left\{ \frac{i}{2^{l_j}} : i = 1, \dots, 2^{l_j-1} \right\}$.

Each set of grids $\Omega_{\underline{l}} \subset \mathbb{R}^d$ is associated with a piecewise d -linear basis function $\phi_{\underline{l}, \underline{h}}(\cdot)$ defined as:

$$\phi_{\underline{l}, \underline{h}}(\mathbf{x}) := \prod_{j=1}^d \phi_{l_j, h_j}(x_j), \quad h_j = 1, \dots, 2^{l_j-1}, \quad \phi_{l_j, h_j}(x) = \begin{cases} 1 - |2^{l_j} x - h_j|, & x \in \left[\frac{h_j-1}{2^{l_j}}, \frac{h_j+1}{2^{l_j}} \right], \\ 0, & \text{otherwise,} \end{cases} \quad (8)$$

where $\mathbf{x} = (x_1, \dots, x_d) \in \mathbb{R}^d$ is a d -dimensional point, $\underline{h} = (h_1, \dots, h_d)$, $\phi_{l_j, h_j}(\cdot)$ is a piecewise linear hierarchical basis shown in [Figure 7a](#).

These basis functions can define function spaces $V_{\underline{l}} := \text{span}\{\phi_{\underline{l},\underline{h}} : h_j = 1, \dots, 2^{l_j} - 1, j = 1, \dots, d\}$ on the grids $\Omega_{\underline{l}}$, then the hierarchical increment spaces $W_{\underline{l}}$ can be defined by

$$W_{\underline{l}} := \text{span}\{\phi_{\underline{l},\underline{h}} : \underline{h} \in B_{\underline{l}}\}, \quad (9)$$

$$B_{\underline{l}} := \{\underline{h} \in \mathbb{N}^d : h_j = 1, \dots, 2^{l_j} - 1, h_j \text{ is odd for all } j = 1, \dots, d\}. \quad (10)$$

Therefore, the function spaces can be represented by the hierarchical increment spaces $V_{\underline{l}} = \bigoplus_{\underline{k} \leq \underline{l}} W_{\underline{k}}$ and each function $f_{\underline{l}} \in V_{\underline{l}}$ can be uniquely represented by $f_{\underline{l}}(\mathbf{x}) = \sum_{|\underline{l}|_1 \leq \eta + d - 1} \sum_{\underline{h} \in B_{\underline{l}}} \alpha_{\underline{l},\underline{h}} \phi_{\underline{l},\underline{h}}(\mathbf{x})$ with hierarchical coefficients $\alpha_{\underline{l},\underline{h}} \in \mathbb{R}$. The space $\bigoplus_{i=1}^n S_i$ is the direct sum of the spaces S_1, \dots, S_n if and only if all nonzero vectors $s_i \in S_i$ (for $i = 1, \dots, n$) are linearly independent, and $\underline{k} \leq \underline{l}$ indicates that each component of \underline{k} is less than or equal to the corresponding component of \underline{l} . The combination technique linearly combines the discrete solutions $f_{\underline{l}}(\mathbf{x})$ from the partial grids $\Omega_{\underline{l}}$ according to the combination formula (see [Figure 7](#)):

$$f_{\eta}^c(\mathbf{x}) = \sum_{\eta \leq |\underline{l}|_1 \leq \eta + d - 1} (-1)^{\eta + d - 1 - |\underline{l}|_1} \binom{d-1}{|\underline{l}|_1 - \eta} f_{\underline{l}}(\mathbf{x}), \quad (11)$$

where the function f_{η}^c is in the sparse grid space $V_{\eta}^s := \bigoplus_{|\underline{l}|_1 \leq \eta + d - 1} W_{\underline{l}}$.

3.2 Optimized combination technique (OptiCom)

Optimized Combination Technique (OptiCom) ([Hegland, 2002](#); [Garcke, 2006](#)) selects the “best possible” combination coefficients adaptively so that an optimal combination approximation is obtained. More specifically, we aim to minimize the functional

$$J(c_1, \dots, c_b) = \|\mathcal{P}_{\eta}^s f - \sum_{i=1}^b c_i \mathcal{P}_i f\|^2, \quad (12)$$

where $\mathcal{P}_{\eta}^s f$ denotes the projection into the sparse grid space V_{η}^s , $\mathcal{P}_i f$ denotes the projection into one of the spaces $V_{\underline{l}}$ in [eq. \(11\)](#), b is the number of summed terms in combination technique formula [eq. \(11\)](#). Using simple expansions and formula $\langle \mathcal{P}_{\eta}^s f, \mathcal{P}_i f \rangle = \langle \mathcal{P}_i f, \mathcal{P}_i f \rangle$, we can obtain

$$J(c_1, \dots, c_b) = \sum_{i,j=1}^b c_i c_j \langle \mathcal{P}_i f, \mathcal{P}_j f \rangle - 2 \sum_{i=1}^b c_i \|\mathcal{P}_i f\|^2 + \|\mathcal{P}_{\eta}^s f\|^2. \quad (13)$$

By differentiating with respect to the combination coefficients c_i and setting each of these derivatives to zero, we can derive the following linear system

$$\begin{bmatrix} \|\mathcal{P}_1 f\|^2 & \cdots & \langle \mathcal{P}_1 f, \mathcal{P}_b f \rangle \\ \langle \mathcal{P}_2 f, \mathcal{P}_1 f \rangle & \cdots & \langle \mathcal{P}_2 f, \mathcal{P}_b f \rangle \\ \vdots & \ddots & \vdots \\ \langle \mathcal{P}_b f, \mathcal{P}_1 f \rangle & \cdots & \|\mathcal{P}_b f\|^2 \end{bmatrix} \begin{bmatrix} c_1 \\ c_2 \\ \vdots \\ c_b \end{bmatrix} = \begin{bmatrix} \|\mathcal{P}_1 f\|^2 \\ \|\mathcal{P}_2 f\|^2 \\ \vdots \\ \|\mathcal{P}_b f\|^2 \end{bmatrix}. \quad (14)$$

Using the optimal coefficients c_i , the OptiCom formula for the sparse grid of level η is then given by

$$f_\eta^c(\mathbf{x}) = \sum_{\eta \leq \|\underline{l}\|_1 \leq \eta + d - 1} c_{\underline{l}} f_{\underline{l}}(\mathbf{x}). \quad (15)$$

For the regression problem (Garcke, 2006), we are seeking the solution of the optimization problem $f^* = \arg \min_{f \in V} R(f)$ with

$$R(f) := \sum_{i=1}^n (f(\mathbf{x}_i) - y_i)^2 + \lambda \|\mathcal{S}f\|_2^2, \quad (16)$$

where \mathcal{S} is a linear operator, λ is the tuning parameter that penalizes the flexibility of the model, $f^* \in V$ is the unknown function we aim to recover from the given dataset $\{(\mathbf{x}_i, y_i)\}_{i=1}^n$, $\mathbf{x}_i \in \mathbb{R}^d$, $y_i \in \mathbb{R}$. The scalar product in the setting is then defined as

$$\langle \mathcal{P}_{\underline{l}} f, \mathcal{P}_{\underline{k}} f \rangle_{\text{RLS}} = \sum_{i=1}^n f_{\underline{l}}(\mathbf{x}_i) f_{\underline{k}}(\mathbf{x}_i) + \lambda \langle \mathcal{S}f_{\underline{l}}, \mathcal{S}f_{\underline{k}} \rangle_2, \quad (17)$$

so that the minimization eq. (16) is an orthogonal projection of f^* into the space V , i.e. if $\|f - f^*\|_{\text{RLS}}^2 \leq \|g - f^*\|_{\text{RLS}}^2$ then $R(f) \leq R(g)$.

3.3 GP with OptiCom

3.3.1 Posterior distribution

It's easy to extend OptiCom to GP regression. Suppose the inducing inputs $\mathbf{Z} = \{\mathbf{z}_i\}_{i=1}^m$ ($\mathbf{z}_i \in \mathbb{R}^d$) are sparse grids Ω_η^d of level η and dimension d defined in eq. (7), then the predictive mean and

covariance in eq. (2) can be approximated in the form

$$\hat{\mu}_\eta^c(\cdot) = \sum_{\eta \leq \|\underline{l}\|_1 \leq \eta + d - 1} c_{\underline{l}} \cdot \sigma_\epsilon^{-2} \mathbf{K}_{(\cdot)\underline{u}_{\underline{l}}} \mathbf{M}_{\underline{u}_{\underline{l}}\underline{u}_{\underline{l}}}^{-1} \mathbf{K}_{\underline{u}_{\underline{l}}\mathbf{f}} \mathbf{y}, \quad (18a)$$

$$\hat{k}_\eta^c(\cdot, \cdot') = \sum_{\eta \leq \|\underline{l}\|_1 \leq \eta + d - 1} (-1)^{\eta + d - 1 - \|\underline{l}\|_1} \binom{d-1}{\|\underline{l}\|_1 - \eta} \left[k(\cdot, \cdot') - \mathbf{K}_{(\cdot)\underline{u}_{\underline{l}}} (\mathbf{K}_{\underline{u}_{\underline{l}}\underline{u}_{\underline{l}}}^{-1} - \mathbf{M}_{\underline{u}_{\underline{l}}\underline{u}_{\underline{l}}}^{-1}) \mathbf{K}_{\underline{u}_{\underline{l}}(\cdot')} \right], \quad (18b)$$

where $\underline{u}_{\underline{l}}$ is the vector of inducing variables corresponding to the inducing inputs $\Omega_{\underline{l}}$ defined in eq. (7), $\mathbf{K}_{(\cdot)\underline{u}_{\underline{l}}} = k(\cdot, \Omega_{\underline{l}}) = \mathbf{K}_{\underline{u}_{\underline{l}}(\cdot)}^\top$, $\mathbf{K}_{\underline{u}_{\underline{l}}\underline{u}_{\underline{l}}} = k(\Omega_{\underline{l}}, \Omega_{\underline{l}})$, and $\mathbf{M}_{\underline{u}_{\underline{l}}\underline{u}_{\underline{l}}} = [\mathbf{K}_{\underline{u}_{\underline{l}}\underline{u}_{\underline{l}}} + \sigma_\epsilon^{-2} \mathbf{K}_{\underline{u}_{\underline{l}}\mathbf{f}} \mathbf{K}_{\mathbf{f}\underline{u}_{\underline{l}}}]$. To ensure that the predictive covariance remains consistent with that of the full GP, we use the CT coefficients rather than those from OptiCom in the covariance computation.

3.3.2 Optimal coefficients

To compute the optimal coefficients $c_{\underline{l}}$ in GP regression, we need to compute the inner product with respect to the *reproducing kernel Hilbert space* (RKHS) (Aronszajn, 1950). Let \mathcal{H} be a RKHS endowed with an inner product $\langle \cdot, \cdot \rangle_{\mathcal{H}}$, then the inner product between functions $f(\cdot) = \sum_{i=1}^n \alpha_i k(\cdot, \mathbf{x}_i)$ and $g(\cdot) = \sum_{j=1}^{n'} \alpha'_j k(\cdot, \mathbf{x}'_j)$ is given by $\langle f, g \rangle_{\mathcal{H}} = \sum_{i=1}^n \sum_{j=1}^{n'} \alpha_i \alpha'_j k(\mathbf{x}_i, \mathbf{x}'_j)$. In GP regression, the optimization problem in eq. (16) becomes $R(f) = \sum_{i=1}^n (f(\mathbf{x}_i) - y_i)^2 + \lambda \|f\|_{\mathcal{H}}^2$, where $\lambda = \sigma_\epsilon^2$ is the noise variance. Here the projection into one of the spaces $V_{\underline{l}}$ has the form

$$\mathcal{P}_{\underline{l}} f = \sigma_\epsilon^{-2} \mathbf{K}_{(\cdot)\underline{u}_{\underline{l}}} \mathbf{M}_{\underline{u}_{\underline{l}}\underline{u}_{\underline{l}}}^{-1} \mathbf{K}_{\underline{u}_{\underline{l}}\mathbf{f}} \mathbf{y} = \sigma_\epsilon^{-2} k(\cdot, \Omega_{\underline{l}}) \boldsymbol{\alpha}_{\underline{l}} = \sigma_\epsilon^{-2} \sum_{i \in \mathbf{I}_{\underline{l}}} k(\cdot, \mathbf{z}_i) \alpha_i := f_{\underline{l}}(\cdot), \quad (19)$$

where $\mathbf{I}_{\underline{l}} \subset \{1, \dots, m\}$ is the set of indices of the inducing inputs $\{\mathbf{z}_i\}_{i=1}^m$ such that $\Omega_{\underline{l}} = \{\mathbf{z}_i : i \in \mathbf{I}_{\underline{l}}\}$, α_i is the i -th component of the vector $\boldsymbol{\alpha}_{\underline{l}} = \mathbf{M}_{\underline{u}_{\underline{l}}\underline{u}_{\underline{l}}}^{-1} \mathbf{K}_{\underline{u}_{\underline{l}}\mathbf{f}} \mathbf{y}$. The scalar product defined in eq. (17) becomes

$$\begin{aligned} \langle \mathcal{P}_{\underline{l}} f, \mathcal{P}_{\underline{k}} f \rangle_{\text{RLS}} &= \sum_{i=1}^n f_{\underline{l}}(\mathbf{x}_i) f_{\underline{k}}(\mathbf{x}_i) + \lambda \langle f_{\underline{l}}, f_{\underline{k}} \rangle_{\mathcal{H}} \\ &= \sigma_\epsilon^{-4} \sum_{i=1}^n k(\mathbf{x}_i, \Omega_{\underline{l}}) \boldsymbol{\alpha}_{\underline{l}}^\top k(\mathbf{x}_i, \Omega_{\underline{k}}) \boldsymbol{\alpha}_{\underline{k}} + \lambda \sigma_\epsilon^{-4} \boldsymbol{\alpha}_{\underline{l}}^\top k(\Omega_{\underline{l}}, \Omega_{\underline{k}}) \boldsymbol{\alpha}_{\underline{k}} \\ &= \sigma_\epsilon^{-2} \boldsymbol{\alpha}_{\underline{l}}^\top [\sigma_\epsilon^{-2} \mathbf{K}_{\underline{u}_{\underline{l}}\mathbf{f}} \mathbf{K}_{\mathbf{f}\underline{u}_{\underline{k}}} + \mathbf{K}_{\underline{u}_{\underline{l}}\underline{u}_{\underline{k}}}] \boldsymbol{\alpha}_{\underline{k}} := \sigma_\epsilon^{-2} \boldsymbol{\alpha}_{\underline{l}}^\top \mathbf{M}_{\underline{u}_{\underline{l}}\underline{u}_{\underline{k}}} \boldsymbol{\alpha}_{\underline{k}}, \end{aligned} \quad (20)$$

where $\mathbf{M}_{\mathbf{u}_l \mathbf{u}_k} = [\mathbf{K}_{\mathbf{u}_l \mathbf{u}_k} + \sigma_\epsilon^{-2} \mathbf{K}_{\mathbf{u}_l \mathbf{f}} \mathbf{K}_{\mathbf{f} \mathbf{u}_k}]$. The details are outlined in [Algorithm 1](#) and [Algorithm 2](#).

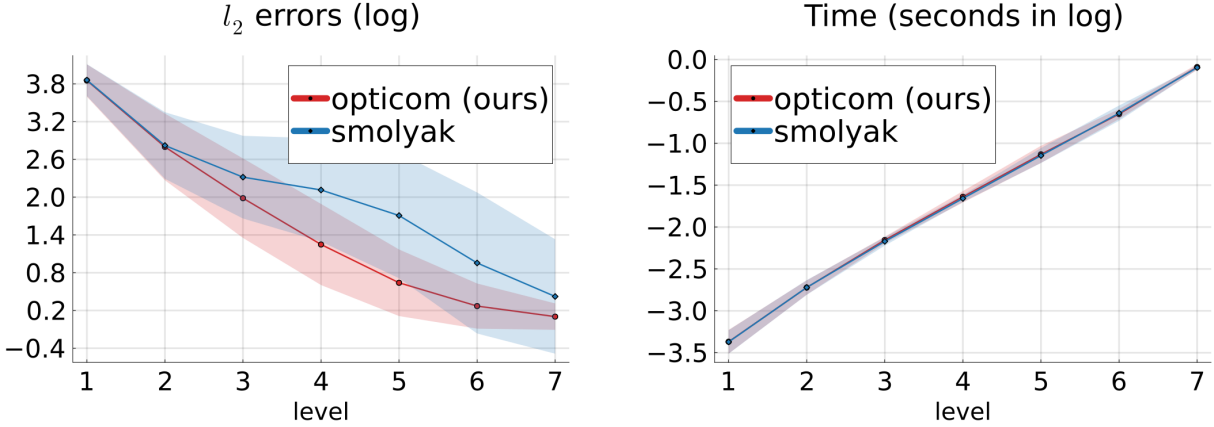


Figure 1: Errors and time for posterior mean of zero mean and Matérn 3/2 GP with OptiCom and CT of dimension $d = 2$ and level $\eta = 1, 2, \dots, 7$ tested on the Griewank function ([Griewank, 1981](#)) over $n = 2000$ training points and $n_t = 1000$ test points. We denote GP with OptiCom by circles and GP with CT by diamonds. *Left:* Logarithm of l_2 errors between GP posteriors and ground truth values averaged over 10 different lengthscales $[0.2, 0.4, 0.6, 0.8, 1.0, 1.2, 1.4, 1.6, 1.8, 2.0]$. *Right:* Logarithm of time taken to compute the posterior mean averaged over 1000 replications.

3.3.3 Complexity

From Lemma 6 in ([Garcke, 2013](#)), we know that the number of summed terms in combination technique formula [eq. \(11\)](#) is $b = \mathcal{O}(\eta^{d-1})$, the size of each summed term is of order $m_b = \mathcal{O}(2^{(\eta+d-1)})$, and dimension of the sparse grid space V_η^s defined in [eq. \(11\)](#), i.e., the number of grid points, is $|V_\eta^s| = \mathcal{O}(2^\eta \cdot \eta^{d-1}) = \mathcal{O}(h_\eta^{-1} \cdot \log(h_\eta^{-1})^{d-1})$, where $h_\eta = 2^{-\eta}$ is the mesh size of the sparse grids Ω_η^d . The additional operations compared to GP with CT include computing $\mathbf{M}_{\mathbf{u}_l \mathbf{u}_k}$ when $l \neq k$ and solving a $b \times b$ linear system to obtain the optimal coefficients, which costs $\mathcal{O}(b^2 m_b^2 n)$ and $\mathcal{O}(b^3)$ time respectively. Note that computation of $\{\mathbf{M}_{\mathbf{u}_l \mathbf{u}_k}\}_{l, k \in \mathbb{I}(\eta, d)}$ and $\{\text{chol}(\mathbf{M}_{\mathbf{u}_l \mathbf{u}_l})\}_{l \in \mathbb{I}(\eta, d)}$ can be parallelized and reduced to $\mathcal{O}(m_b^2 n)$ time and $\mathcal{O}(m_b^3)$ time respectively, where $\mathbb{I}(\eta, d) = \{l : \eta \leq |l|_1 \leq \eta + d - 1\}$. Thus the computational complexity of the parallelized [Algorithm 2](#) is $\mathcal{O}(m_b^3 + b^3 + m_b^2 n) = \mathcal{O}(b^3 + m_b^2 n)$. Although the computational complexity of the parallelized GP with OptiCom is larger than that of parallelized GP with CT theoretically, which is $\mathcal{O}(m_b^2 n)$, b is very small in most cases, hence $\mathcal{O}(b^3 + m_b^2 n) \approx \mathcal{O}(m_b^2 n)$. [Figure 1](#) also demonstrates that GP with OptiCom achieves lower errors and smaller variance than GP with CT at nearly the same time cost.

4 Distributed GP with optimal weights

In our previous formulation of GP with OptiCom, the inducing points were placed on fixed sparse grids rather than being learned through variational inference. While this design simplifies computation, it can limit performance when the sparse grid resolution is low, as the fixed locations may not adequately capture complex input structures. To address this limitation, we extend OptiCom to distributed GPs, which allows for greater flexibility and improved accuracy while maintaining computational efficiency and does not rely on sparse grid structures. Following the assumptions [Section 2.2.1](#), we consider the global training dataset $\mathcal{D} = \{\mathbf{X}, \mathbf{y}\}$ of size n , partitioned into M local datasets $\mathcal{D}_i = \{\mathbf{X}_i, \mathbf{y}_i\}$ of size n_i for $i = 1, \dots, M$. All the local datasets are assumed to share the same hyperparameters θ .

4.1 Distributed SVGP

4.1.1 Optimal weights

To obtain the optimal weights, as shown the [eq. \(12\)](#) and [eq. \(13\)](#) in [Section 3.2](#), the objective is to minimize

$$J(\beta_1, \dots, \beta_M) = \|f - \sum_{i=1}^M \beta_i \mathcal{P}_i f\|, \quad (21)$$

where $f(\cdot) \sim \mathcal{GP}(0, k(\cdot, \cdot))$ as defined in [Section 2.2.1](#), $\mathcal{P}_i f = f|_{\mathbf{y}_i} := f_i$ is the posterior conditioned on the local dataset $\mathcal{D}_i = \{\mathbf{X}_i, \mathbf{y}_i\}$, and its distribution takes the form of [eq. \(2\)](#). Similar to [Section 3.3](#), the optimal weights $\{\beta_i\}_{i=1}^M$ can be obtained by solving the following linear system:

$$\begin{bmatrix} \|\mathcal{P}_1 f\|^2 & \cdots & \langle \mathcal{P}_1 f, \mathcal{P}_M f \rangle \\ \langle \mathcal{P}_2 f, \mathcal{P}_1 f \rangle & \cdots & \langle \mathcal{P}_2 f, \mathcal{P}_M f \rangle \\ \vdots & \ddots & \vdots \\ \langle \mathcal{P}_M f, \mathcal{P}_1 f \rangle & \cdots & \|\mathcal{P}_M f\|^2 \end{bmatrix} \begin{bmatrix} \beta_1 \\ \beta_2 \\ \vdots \\ \beta_M \end{bmatrix} = \begin{bmatrix} \|\mathcal{P}_1 f\|^2 \\ \|\mathcal{P}_2 f\|^2 \\ \vdots \\ \|\mathcal{P}_M f\|^2 \end{bmatrix}. \quad (22)$$

To reduce computational complexity, we randomly select a central dataset $\mathcal{D}_c := \{\mathbf{X}_c, \mathbf{y}_c\} \subset \mathcal{D} = \{\mathbf{X}, \mathbf{y}\}$ of size $n_c \ll n$. In practice, we select one point from each local dataset \mathcal{D}_i and combine them to form the central dataset, resulting in $n_c = M$. Consequently, the scalar product is approximated

as follows:

$$\begin{aligned}
\langle \mathcal{P}_l f, \mathcal{P}_k f \rangle_{\text{RLS}} &= \sum_{\mathbf{x}_i \in \mathbf{X}} f_l(\mathbf{x}_i) f_k(\mathbf{x}_i) + \lambda \langle f_l, f_k \rangle_{\mathcal{H}} \\
&\approx \sum_{\mathbf{x}_i \in \mathbf{X}_c} f_l(\mathbf{x}_i) f_k(\mathbf{x}_i) + \lambda \langle f_l, f_k \rangle_{\mathcal{H}} \\
&= \sigma_\epsilon^{-2} \boldsymbol{\alpha}_l^\top [\sigma_\epsilon^{-2} \mathbf{K}_{\text{uf}_c} \mathbf{K}_{\text{f}_c \text{u}} + \mathbf{K}_{\text{uu}}] \boldsymbol{\alpha}_k := \sigma_\epsilon^{-2} \boldsymbol{\alpha}_l^\top \mathbf{M}_{\text{uu}}^{(c)} \boldsymbol{\alpha}_k,
\end{aligned} \tag{23}$$

where $\boldsymbol{\alpha}_l = [\mathbf{M}_{\text{uu}}^{(l)}]^{-1} \mathbf{K}_{\text{uf}_l} \mathbf{y}_l$, $\mathbf{M}_{\text{uu}}^{(l)} = [\mathbf{K}_{\text{uu}} + \sigma_\epsilon^{-2} \mathbf{K}_{\text{uf}_l} \mathbf{K}_{\text{f}_l \text{u}}]$, $\mathbf{K}_{\text{uu}} = k(\mathbf{Z}, \mathbf{Z})$, $\mathbf{K}_{\text{uf}_l} = k(\mathbf{Z}, \mathbf{X}_l) = \mathbf{K}_{\text{f}_l \text{u}}^\top$, $\mathbf{M}_{\text{uu}}^{(c)} = [\mathbf{K}_{\text{uu}} + \sigma_\epsilon^{-2} \mathbf{K}_{\text{uf}_c} \mathbf{K}_{\text{f}_c \text{u}}]$, $\mathbf{K}_{\text{uf}_c} = k(\mathbf{Z}, \mathbf{X}_c) = \mathbf{K}_{\text{f}_c \text{u}}^\top$, $\mathbf{Z} = \{\mathbf{z}_i\}_{i=1}^m$ are the inducing inputs corresponding to the optimized inducing variables $\mathbf{u} \in \mathbb{R}^m$. The details are outlined in [Algorithm 3](#).

In addition, the optimal weights computed in [eq. \(22\)](#) inherently capture the correlations between local experts. This mechanism prevents redundant information from being overemphasized when experts are highly correlated, thus leading to a more balanced aggregation. As a result, the aggregated prediction becomes more consistent with that of a full GP. This integration of expert correlations is key to enhancing both the performance and stability of distributed GP.

4.1.2 Aggregated prediction

Instead of relying on PoE-based models, we directly use the optimal weights $\{\beta_i\}_{i=1}^M$ to predict the aggregated GP models after distributed training. Note that the correlations between the experts are already incorporated into the optimal weights. Therefore, we use the weighted local variances to approximate the aggregated variance, reducing computational complexity. The joint mean and joint variance are given as follows:

$$\mu_{\mathcal{A}}(\cdot) = \sum_{i=1}^M \beta_i \mathbb{E}[f_i(\cdot)] = \sum_{i=1}^M \beta_i \sigma_\epsilon^{-2} \mathbf{K}_{(\cdot) \text{u}} \mathbf{M}_{\text{uu}}^{(i)-1} \mathbf{K}_{\text{uf}_i} \mathbf{y}_i, \tag{24a}$$

$$\sigma_{\mathcal{A}}^2(\cdot) = \sum_{i=1}^M \beta_i^2 \text{Var}[f_i(\cdot), f_i(\cdot)] = \sum_{i=1}^M \beta_i^2 \mathbf{K}_{(\cdot) \text{u}} [\mathbf{M}_{\text{uu}}^{(i)}]^{-1} \mathbf{K}_{\text{u}(\cdot)}, \tag{24b}$$

The details are outlined in [Algorithm 4](#).

4.1.3 Complexity

In [Algorithm 3](#), the computation of $\{\mathbf{M}_{\mathbf{u}\mathbf{u}}^{(i)}\}_{i=1}^M$ and $\{\text{chol}(\mathbf{M}_{\mathbf{u}\mathbf{u}}^{(i)})\}_{i=1}^M$ requires $\mathcal{O}(m^2n_i)$ time and $\mathcal{O}(m^3)$ time, respectively, after parallelization, and solving the $M \times M$ linear system costs $\mathcal{O}(M^3)$ time. Therefore, the time complexity of the parallelized [Algorithm 3](#) is $\mathcal{O}(m^2n_i + m^3 + M^3) = \mathcal{O}(m^2n_i + M^3)$. For the aggregated prediction, the computational complexity of the joint mean and joint variance is $\mathcal{O}(M)$. Thus, the computational complexity of the parallelized [Algorithm 4](#) is $\mathcal{O}(m^2n_i + M^3 + M) = \mathcal{O}(m^2n_i + M^3)$, where m is the size of shared inducing variables \mathbf{u} across the experts $\{\mathcal{M}_i\}_{i=1}^M$, n_i is the size of the local dataset \mathcal{D}_i for expert \mathcal{M}_i , ($i = 1, \dots, M$), and M is the number of experts. The comparison of the time complexity of the aggregation models and full SVGP is presented in the first row of [Table 1](#).

Table 1: Complexity of the prediction for aggregation models. m is the number of inducing points, n is the size of the entire training dataset, n_i is the size of the local dataset \mathcal{D}_i corresponding to the expert \mathcal{M}_i , $i = 1, \dots, M$, n_c is the size of the dataset \mathcal{D}_c corresponding to the expert \mathcal{M}_c for grBCM. M is the number of experts.

		PoE	gPoE	BCM	rBCM	grBCM	NPAE	opt (ours)
Time	SVGP	$\mathcal{O}(m^2n_i + M)$	$\mathcal{O}(m^2n_i + M)$	$\mathcal{O}(m^2n_i + M)$	$\mathcal{O}(m^2n_i + M)$	$\mathcal{O}(m^2(n_i + n_c) + M)$	$\mathcal{O}(m^2n_iM + M^3)$	$\mathcal{O}(m^2n_i + M^3)$
	ExactGP	$\mathcal{O}(n_i^3 + M)$	$\mathcal{O}(n_i^3 + M)$	$\mathcal{O}(n_i^3 + M)$	$\mathcal{O}(n_i^3 + M)$	$\mathcal{O}((n_i + n_c)^3 + M)$	$\mathcal{O}(n_i^3M + M^3)$	$\mathcal{O}(n_i^3 + M^3)$

4.2 Distributed exact GP

The optimal weights method for distributed GPs is also applicable to exact GPs. In this case, the distribution of $\mathcal{P}_i f = f | \mathbf{y}_i := f_i$ follows the form given in [eq. \(1\)](#). Consequently, the scalar product is expressed as:

$$\begin{aligned}
 \langle \mathcal{P}_l f, \mathcal{P}_k f \rangle_{\text{RLS}} &\approx \sum_{\mathbf{x}_i \in \mathbf{X}_c} f_l(\mathbf{x}_i) f_k(\mathbf{x}_i) + \lambda \langle f_l, f_k \rangle_{\mathcal{H}} \\
 &= \boldsymbol{\alpha}_l^\top [\mathbf{K}_{\mathbf{f}_l \mathbf{f}_c} \mathbf{K}_{\mathbf{f}_c \mathbf{f}_k} + \mathbf{K}_{\mathbf{f}_l \mathbf{f}_k}] \boldsymbol{\alpha}_k := \boldsymbol{\alpha}_l^\top \mathbf{M}_{\mathbf{f}_l \mathbf{f}_k}^{(c)} \boldsymbol{\alpha}_k,
 \end{aligned} \tag{25}$$

where $\boldsymbol{\alpha}_l = \tilde{\mathbf{K}}_{\mathbf{f}_l \mathbf{f}_l}^{-1} \mathbf{y}_l$, $\tilde{\mathbf{K}}_{\mathbf{f}_l \mathbf{f}_l} = \mathbf{K}_{\mathbf{f}_l \mathbf{f}_l} + \sigma_\epsilon^2 \mathbf{I}_{n_l}$, $\mathbf{M}_{\mathbf{f}_l \mathbf{f}_k}^{(c)} = [\mathbf{K}_{\mathbf{f}_l \mathbf{f}_k} + \mathbf{K}_{\mathbf{f}_l \mathbf{f}_c} \mathbf{K}_{\mathbf{f}_c \mathbf{f}_k}]$, $\mathbf{K}_{\mathbf{f}_l \mathbf{f}_k} = k(\mathbf{X}_l, \mathbf{X}_k)$. Therefore, the joint mean and joint variance are given by:

$$\mu_{\mathcal{A}}(\cdot) = \sum_{i=1}^M \beta_i \mathbf{K}_{(\cdot) \mathbf{f}_i} \tilde{\mathbf{K}}_{\mathbf{f}_i \mathbf{f}_i}^{-1} \mathbf{y}_i, \quad \sigma_{\mathcal{A}}^2(\cdot) = \sum_{i=1}^M \beta_i^2 \mathbf{K}_{(\cdot) \mathbf{f}_i} \tilde{\mathbf{K}}_{\mathbf{f}_i \mathbf{f}_i}^{-1} \mathbf{K}_{\mathbf{f}_i (\cdot)}. \tag{26}$$

The detailed procedures are outlined in [Algorithm 5](#) and [Algorithm 6](#). The time complexity of the parallelized [Algorithm 6](#) is $\mathcal{O}(n_i^3 + M^3)$, where n_i is the size of the local dataset \mathcal{D}_i for expert \mathcal{M}_i , and M is the number of experts. A comparison of the time complexity of the aggregation models and the full exact GP is presented in the last row of [Table 1](#).

4.3 Convergence

In this section, we introduce the theoretical properties of the proposed aggregation method with optimal weights. In contrast to PoE and BCM families whose weights are chosen heuristically, our weights are defined as the minimizer of a function space residual objective in [eq. \(21\)](#) and are computed from the resulting linear system in [eq. \(22\)](#). This optimization-based method is what enables the consistency for the aggregated predictor.

Setting. Let the global dataset \mathcal{D} be randomly partitioned into local datasets $\{\mathcal{D}_i\}_{i=1}^{M_n}$ without replacement, where the number of experts M_n increases with the global dataset size n such that (i) $\lim_{n \rightarrow \infty} M_n = \infty$, and (ii) $\liminf_{n \rightarrow \infty} \frac{n}{M_n^2} > 0$. Then the local sample sizes satisfy $n_i \asymp n/M_n \rightarrow \infty$. Assume each expert \mathcal{M}_i is a zero-mean GP with the same kernel and Gaussian noise model as the full GP.

For each GP expert, let $\mathcal{P}_i f$ denote the posterior operator conditioned on the local dataset \mathcal{D}_i (as defined in [eq. \(21\)](#)). Let $\mu_i(\cdot)$ and $\sigma_i^2(\cdot)$ be the predictive mean and variance of expert i , where $i = 1, \dots, M_n$, and let $\mu_{\text{full}}(\cdot)$ and $\sigma_{\text{full}}^2(\cdot)$ denote the predictive mean and variance of the full GP trained on \mathcal{D} .

Assumptions.

1. local predictive consistency.

We assume a standard GP predictive consistency property: as the local sample size $n_i \rightarrow \infty$, the predictive mean and variance of the i -th expert converge to the same limiting predictive quantities as the full GP, at any fixed test input \mathbf{x}_* . This is a classical result in GP posterior consistency theory ([Choi, 2005](#)), and it is also the auxiliary fact from proof of Proposition 2 in ([Liu et al., 2018](#)) to control the asymptotic behavior of each expert’s predictive mean and

variance. Specifically, for any fixed \mathbf{x}_* ,

$$\lim_{n \rightarrow \infty} \max_{1 \leq i \leq M_n} |\mu_i(\mathbf{x}_*) - \mu_{\text{full}}(\mathbf{x}_*)| = 0, \quad \lim_{n \rightarrow \infty} \max_{1 \leq i \leq M_n} |\sigma_i^2(\mathbf{x}_*) - \sigma_{\text{full}}^2(\mathbf{x}_*)| = 0. \quad (27)$$

2. weight stability.

We assume the optimizer $\boldsymbol{\beta}_n = (\beta_{1,n}, \dots, \beta_{M_n,n})^\top$ returned by the linear system in eq. (22) is stable, i.e.:

$$\|\boldsymbol{\beta}_n\|_{\ell_1} \leq B \quad \text{for all sufficiently large } n, \quad (28)$$

for some constant B independent of n . This assumption is standard for linear estimators: without controlling the magnitude of $\boldsymbol{\beta}_n$, the residual term $\sum_{i=1}^{M_n} \beta_{i,n}(f - \mathcal{P}_i f)$ below may fail to vanish even if each $(f - \mathcal{P}_i f) \rightarrow 0$. In practice, such stability can be enforced by adding a small jitter regularizer to the Gram matrix in eq. (22).

Aggregation prediction. The aggregated predictor of the proposed method has the form (see eqs. (24) and (26))

$$\mu_{\mathcal{A}}(\mathbf{x}_*) = \sum_{i=1}^{M_n} \beta_{i,n} \mu_i(\mathbf{x}_*), \quad \sigma_{\mathcal{A}}^2(\mathbf{x}_*) = \sum_{i=1}^{M_n} \beta_{i,n}^2 \sigma_i^2(\mathbf{x}_*). \quad (29)$$

Define the sum of weights $s_n := \sum_{i=1}^{M_n} \beta_{i,n}$, then we have the decomposition as follows:

$$\mu_{\mathcal{A}}(\mathbf{x}_*) = s_n \mu_{\text{full}}(\mathbf{x}_*) + \sum_{i=1}^{M_n} \beta_{i,n} (\mu_i(\mathbf{x}_*) - \mu_{\text{full}}(\mathbf{x}_*)). \quad (30)$$

Thus, mean consistency reduces to proving (i) $s_n \rightarrow 1$, and (ii) the second term in eq. (30) converges to zero.

Mean.

- **Step 1: the objective value at the optimizer converges to zero.**

Define the function space residual objective from eq. (21)

$$J_n(\boldsymbol{\beta}) := \left\| f - \sum_{i=1}^{M_n} \beta_i \mathcal{P}_i f \right\|. \quad (31)$$

Let β_n be a minimizer of $J_n(\beta)$. Then for any $j \in \{1, \dots, M_n\}$,

$$J_n(\beta_n) \leq J_n(\mathbf{e}_j) = \|f - \mathcal{P}_j f\|, \quad (32)$$

where \mathbf{e}_j is the j -th standard basis vector. By Assumption 1 and $n_j \asymp n/M_n \rightarrow \infty$, we have

$$\lim_{n \rightarrow \infty} \|f - \mathcal{P}_j f\| = 0 \quad (33)$$

Therefore,

$$\lim_{n \rightarrow \infty} J_n(\beta_n) = 0 \quad (34)$$

- **Step 2: derive** $s_n = \sum_{i=1}^{M_n} \beta_{i,n} \rightarrow 1$.

Using the identity

$$f - \sum_{i=1}^{M_n} \beta_{i,n} \mathcal{P}_i f = (1 - s_n)f + \sum_{i=1}^{M_n} \beta_{i,n} (f - \mathcal{P}_i f), \quad (35)$$

we bound $|1 - s_n|$ by applying the triangle inequality:

$$\begin{aligned} |1 - s_n| \cdot \|f\| &= \|(1 - s_n)f\| \\ &\leq \left\| f - \sum_{i=1}^{M_n} \beta_{i,n} \mathcal{P}_i f \right\| + \left\| \sum_{i=1}^{M_n} \beta_{i,n} (f - \mathcal{P}_i f) \right\| \\ &\leq J_n(\beta_n) + \sum_{i=1}^{M_n} |\beta_{i,n}| \cdot \|f - \mathcal{P}_i f\| \\ &\leq J_n(\beta_n) + \|\beta_n\|_{\ell_1} \max_{1 \leq i \leq M_n} \|f - \mathcal{P}_i f\|. \end{aligned} \quad (36)$$

By eq. (34), the first term $J_n(\beta_n)$ tends to 0. By Assumption 1, $\lim_{n \rightarrow \infty} \max_i \|f - \mathcal{P}_i f\| = 0$, and by Assumption 2, $\|\beta_n\|_{\ell_1} \leq B$. Hence the right hand side of eq. (36) converges to 0, which implies that

$$\lim_{n \rightarrow \infty} \sum_{i=1}^{M_n} \beta_{i,n} = \lim_{n \rightarrow \infty} s_n = 1. \quad (37)$$

- **Step 3: prove mean consistency.** Return to eq. (30). The second term is bounded by

$$\left| \sum_{i=1}^{M_n} \beta_{i,n} (\mu_i(\mathbf{x}_*) - \mu_{\text{full}}(\mathbf{x}_*)) \right| \leq \|\boldsymbol{\beta}_n\|_{\ell_1} \max_{1 \leq i \leq M_n} |\mu_i(\mathbf{x}_*) - \mu_{\text{full}}(\mathbf{x}_*)| \rightarrow 0 \quad \text{as } n \rightarrow \infty \quad (38)$$

using eqs. (27) and (28). Combining this with eq. (37) yields

$$\lim_{n \rightarrow \infty} \mu_{\mathcal{A}}(\mathbf{x}_*) = \lim_{n \rightarrow \infty} \left(s_n \mu_{\text{full}}(\mathbf{x}_*) + \sum_{i=1}^{M_n} \beta_{i,n} (\mu_i(\mathbf{x}_*) - \mu_{\text{full}}(\mathbf{x}_*)) \right) \quad (39)$$

$$= 1 \cdot \mu_{\text{full}}(\mathbf{x}_*) + 0 \quad (40)$$

$$= \mu_{\text{full}}(\mathbf{x}_*). \quad (41)$$

Therefore, the aggregated predictive mean is consistent.

Variance. Using eq. (29) we get the following decomposition for aggregated predictive variance:

$$\begin{aligned} \sigma_{\mathcal{A}}^2(\mathbf{x}_*) &= \sum_{i=1}^{M_n} \beta_{i,n}^2 \sigma_i^2(\mathbf{x}_*) \\ &= \left(\sum_{i=1}^{M_n} \beta_{i,n}^2 \right) \sigma_{\text{full}}^2(\mathbf{x}_*) + \sum_{i=1}^{M_n} \beta_{i,n}^2 (\sigma_i^2(\mathbf{x}_*) - \sigma_{\text{full}}^2(\mathbf{x}_*)). \end{aligned} \quad (42)$$

If $\|\boldsymbol{\beta}_n\|_{\ell_2}$ is uniformly bounded, then the second term in eq. (42) goes to zero by Assumption 1. However, to obtain $\sigma_{\mathcal{A}}^2(\mathbf{x}_*) \rightarrow \sigma_{\text{full}}^2(\mathbf{x}_*)$ one further needs the stronger condition $\sum_i \beta_{i,n}^2 \rightarrow 1$, which we do not enforce. Consequently, our theoretical guarantee is primarily for the predictive mean, while variance consistency would require additional constraints on $\boldsymbol{\beta}_n$.

Stability. Assumption 2 is required for a rigorous argument, i.e., the term $\sum_i \beta_{i,n} (f - \mathcal{P}_i f)$ in eq. (35) may not vanish without controlling the magnitude of $\boldsymbol{\beta}_n$ even when each component $(f - \mathcal{P}_i f) \rightarrow 0$. In our method, $\boldsymbol{\beta}_n$ is obtained by solving the finite dimensional linear system eq. (22) derived from the first-order optimality conditions of the function space objective $J_n(\boldsymbol{\beta})$. The solution is stable whenever the corresponding Gram matrix is well-conditioned. In practice, we ensure numerical stability by adding a small jitter to eq. (22), which is standard in GP computations and typically yields bounded solutions.

5 Experiments

In this section, we evaluate the proposed algorithm against full GP and several baselines that aggregate predictions via weighted averaging: PoE, gPoE, BCM, rBCM, and grBCM, using both synthetic data (Section 5.1) and UCI datasets (Asuncion and Newman, 2007) (Section 5.2). We restrict baselines to aggregation methods because our contribution is an aggregation algorithm for distributed GP experts, scalable methods for centralized GP such as inducing points approximations, structured kernel interpolation, Vecchia framework, or stochastic dual descent solvers are complementary and can be used within each expert, but they do not provide a competing aggregation mechanism under the distributed learning setting. The size of the inducing variables is set to $m = 128$. We use the *radial basis function* (RBF) kernel with separate lengthscales l_i for each input dimension i , and $\sigma_f^2 > 0$ is the signal variance of the kernel. The code for the experiments is available at <https://github.com/hchen19/optimal-distgp>.

5.1 Synthetic data

5.1.1 Training

In this section, we assess the performance of four distributed training methods for SVGP: FACT, ADMM, FedAvg, and FedProx. We generate a training dataset of size $n = 10^4$ and dimension $d = 2$ using the RBF kernel with $(l_1, l_2, \sigma_\epsilon, \sigma_f) = (0.3, 1.3, 0.1, 0.2)$. The dataset is distributed among $M = 2, 4, 8, 10, 20, 40, 80, 100$ experts, respectively. We set the initial values of the hyperparameters $(l_1^{(0)}, l_2^{(0)}, \sigma_\epsilon^{(0)}, \sigma_f^{(0)}) = (2.0, 0.3, 1.0, \sqrt{1.5})$, and use Adam optimizer (Kingma and Ba, 2015) with a learning rate of 0.1 for all methods. For ADMM, the regularization parameter is set to $\rho = 500$. For FedProx, the proximal coefficient is set to $\mu = 0.01$, with a sampling rate of 0.5 for the local updates. The hyperparameters of the SVGP $\theta = (l_1, l_2, \sigma_\epsilon, \sigma_f, \mathbf{u})^\top$ are trained over 200 iterations, where \mathbf{u} are the inducing variables of size $m = 128$. The results are averaged over 10 different seeds for each setting of M .

Figure 2 illustrates the change of the parameters with the training iterations for different numbers of experts M . We observe that FACT and ADMM perform worse as the number of experts M increases, while FedAvg performs the best overall, converging faster and more stably than FedProx. Figure 8 shows boxplots of the hyperparameter estimates after 200 iterations, indicating that FedAvg converges closest to the ground truth with the least variability. Therefore, we use FedAvg for

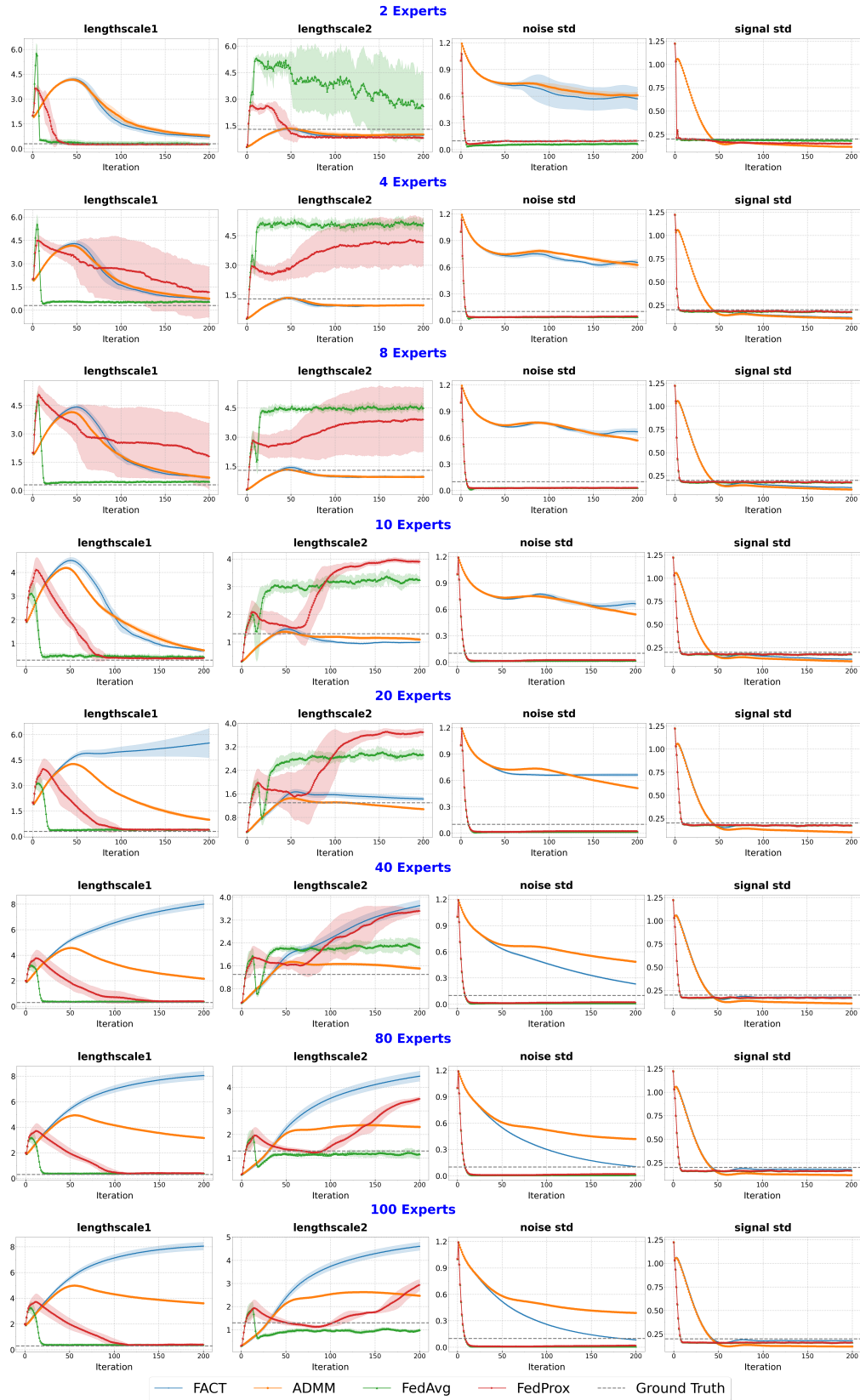


Figure 2: Hyperparameter estimates versus the training iterations on the $n = 10^4$ dataset.

distributed training in the experiments with the UCI datasets.

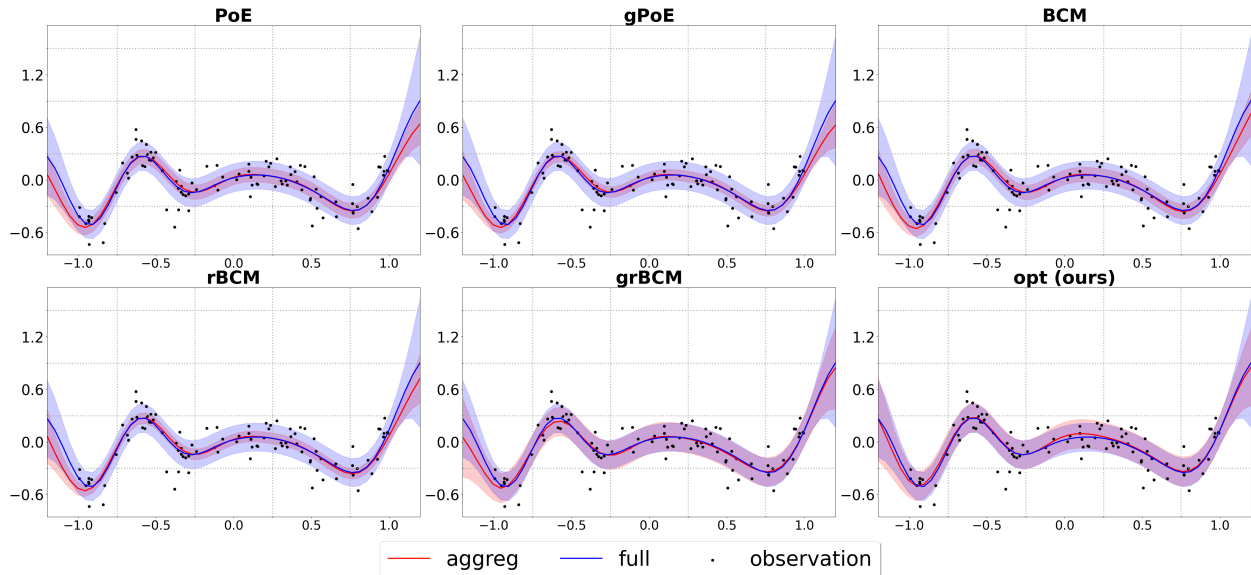


Figure 3: SVGP posteriors with the different aggregation models on $n = 100$ training points in $[-1, 1]$ and $n_t = 50$ test points in $[-1.2, 1.2]$ with the number of experts $M = 4$, dimension $d = 1$, and the number of inducing variables $m = 128$. We denote the aggregated predictions (aggreg) by dashed lines, the full SVGP posteriors (full) by solid lines, and the observations by dots.

5.1.2 Prediction

In this section, we evaluate the performance of aggregation models and full GP models without optimizing any hyperparameters. We generate the ground truth dataset using RBF kernel with fixed hyperparameters $(l_i, \sigma_\epsilon^2, \sigma_f^2) = (0.3, 0.25, 1.0)$ for all $i = 1, \dots, d$. For SVGP, we use $m = 128$ inducing points, randomly generated with a fixed seed across all aggregation methods.

Figure 3 shows the aggregated predictions of SVGP on $n = 100$ training points uniformly sampled in $[-1, 1]$ and $n_t = 50$ test points evenly spaced in $[-1.2, 1.2]$, with dimension $d = 1$ and $M = 4$ experts. We compare our method (opt) against five baselines (PoE, gPoE, BCM, rBCM, grBCM) and the full SVGP model using the same inducing points. The proposed method yields predictions that closely match the full SVGP, especially in the extrapolation region outside the training domain (i.e., in $[-1.2, -1] \cup [1, 1.2]$). In contrast, most baselines show degraded performance in these regions. Furthermore, the predictive variances of our method and grBCM align more closely with the full SVGP, suggesting better consistency of the predictions compared to other methods.

Next, we evaluate the aggregation models on $n = 10^4$ training data of dimension $d = 2$ in $[-1, 1]^2$ and $n_t = 50 \times 50 = 2500$ test points, evenly spaced over the interval $[-1.2, 1.2]^2$. The

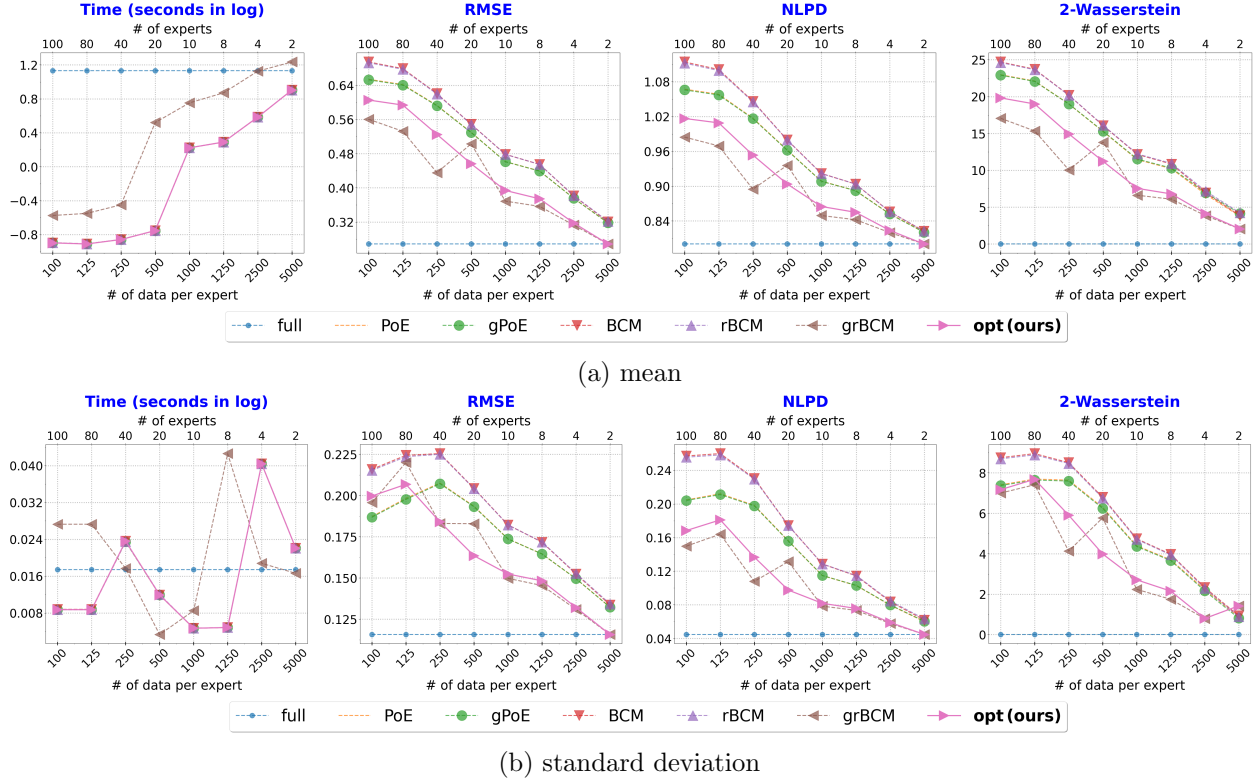


Figure 4: Comparison of the aggregation models for **Exact GP** with the RBF kernel in dimension $d = 2$ on $n = 10^4$ training points in $[-1, 1]^2$ and $n_t = 2500$ test points in $[-1.2, 1.2]^2$. The number of experts considered are $M = 2, 4, 8, 10, 20, 40, 80, 100$. The lower x -axis represents the size of the local training dataset $n_i = n/M$, and the upper x -axis represents the number of the experts M . *Left*: Logarithm of time for computing the aggregated predictions. *Middle Left*: RMSE between the aggregated predictions and the ground truth. *Middle Right*: NLPD between the aggregated predictions and the ground truth. *Right*: 2-Wasserstein distance to the full GP. *Top*: Mean of the computational time, RMSE, NLPD, and 2-Wasserstein distance. *Bottom*: Standard deviation of the computational time, RMSE, NLPD, and 2-Wasserstein distance.

training dataset is divided among $M = 2, 4, 8, 10, 20, 40, 80, 100$ experts, respectively. To eliminate the impact of seeds, we average all the metrics over 10 different seeds for each setting of M .

Figure 4 compares the performance of various aggregation models for exact GPs using four metrics: computational time, *root mean squared error* (RMSE), *negative log predictive density* (NLPD), and 2-Wasserstein distance to the full exact GP (measuring how closely each aggregated model approximates the full GP). While grBCM performs the best in RMSE, NLPD, and 2-Wasserstein distance, it requires more computational time due to the larger size of the augmented local training datasets and has larger standard deviations of the metrics. Our method, GP with optimal weights, provides comparable predictions with significantly lower computational cost. Figure 5 also compares four metrics for SVGP across all aggregation models. It’s observed that our method and grBCM

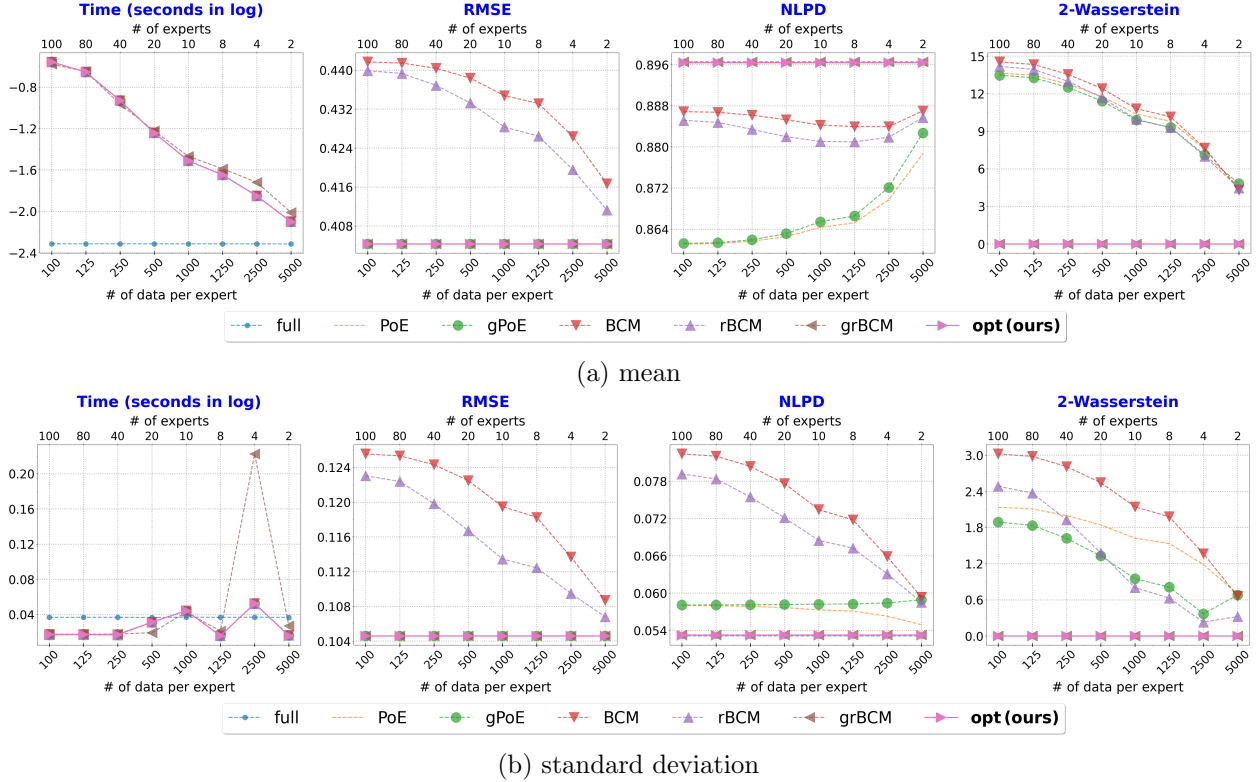


Figure 5: Comparison of the aggregation models for **SVGP** with the RBF kernel in dimension $d = 2$ on $n = 10^4$ training points in $[-1, 1]^2$, $m = 128$ inducing points, and $n_t = 2500$ test points in $[-1.2, 1.2]^2$. The number of experts considered are $M = 2, 4, 8, 10, 20, 40, 80, 100$. The lower x -axis represents the size of the local training dataset $n_i = n/M$, and the upper x -axis represents the number of the experts M . *Left*: Logarithm of time for computing the aggregated predictions. *Middle Left*: RMSE between the aggregated predictions and the ground truth. *Middle Right*: NLPD between the aggregated predictions and the ground truth. *Right*: 2-Wasserstein distance to the full GP. *Top*: Mean of the computational time, RMSE, NLPD, and 2-Wasserstein distance. *Bottom*: Standard deviation of the computational time, RMSE, NLPD, and 2-Wasserstein distance.

significantly outperform other methods for SVGP.

5.2 UCI regression for temporal extrapolation

In this section, we evaluate the aggregation models on three real-world time-series datasets from the UCI repository (Asuncion and Newman, 2007): Gas Turbine CO and NO_x Emission (Kaya et al., 2019), Beijing PM_{2.5} (Liang et al., 2015), and Metro Interstate Traffic Volume (Hogue, 2019). Unlike standard random train-test splits, we employ *temporal extrapolation splits* where models are trained on earlier years and tested on future years, creating a more realistic and challenging evaluation scenario that tests the models' ability to handle distribution shift and regime changes.

Dataset descriptions and splits:

- **Gas Turbine CO & NOx** (36,733 samples, 10 features): Hourly sensor measurements from 2011–2015. Training on 2011–2013, testing on 2014–2015. This dataset contains two prediction targets: CO and NOx emissions, we run experiments independently for each target. The future years contain operational regimes not fully represented in training data.
- **Beijing PM2.5** (43,824 samples, 13 features): Hourly air quality measurements from 2010–2014. Training on 2010–2013, testing on 2014. The test period includes extreme pollution events such as haze episodes that challenge model calibration.
- **Metro Traffic** (48,204 samples, 8 features): Hourly traffic volume measurements from 2012–2018. Training on 2012–2016, testing on 2017–2018. Traffic patterns exhibit regime shifts from construction, policy changes, and seasonal variations.

Experimental setup: To create a challenging distributed setting where expert diversity and correlation become important, we partition each training dataset into $M = 20, 40, 60$ heterogeneous experts by randomly shuffling and dividing the data. Specifically, we use **non-shared hyperparameters** across experts (i.e., each expert optimizes its own lengthscale, kernel variance, and noise variance independently), which creates the strong correlated local datasets that our method can handle. We employ SVGP with $m = 128$ inducing points and RBF kernel. All aggregation models utilize FedAvg with the Adam optimizer, with 500 training iterations to ensure sufficient convergence for the extrapolation task. Results are averaged over 10 different random seeds.

Figure 6 presents the performance metrics of the aggregation models on these four datasets. It’s observed that: (1) BCM and rBCM perform poorly, particularly for NOx and Beijing PM2.5, where it yields significantly degraded RMSE and NLPD due to overconfident but incorrect experts being equally weighted. (2) While grBCM shows competitive RMSE, it requires substantially more computation time due to the need to train additional models. (3) Our method, distributed SVGP with optimal weights (opt), consistently achieves the best or near-best RMSE and NLPD across all datasets while maintaining computational efficiency comparable to simpler baselines. Notably, on the challenging extrapolation tasks (NOx and Metro Traffic), our method’s ability to account for expert correlation and reliability provides clear advantages in both prediction accuracy and uncertainty quantification. Detailed metric values are reported in Table 2.

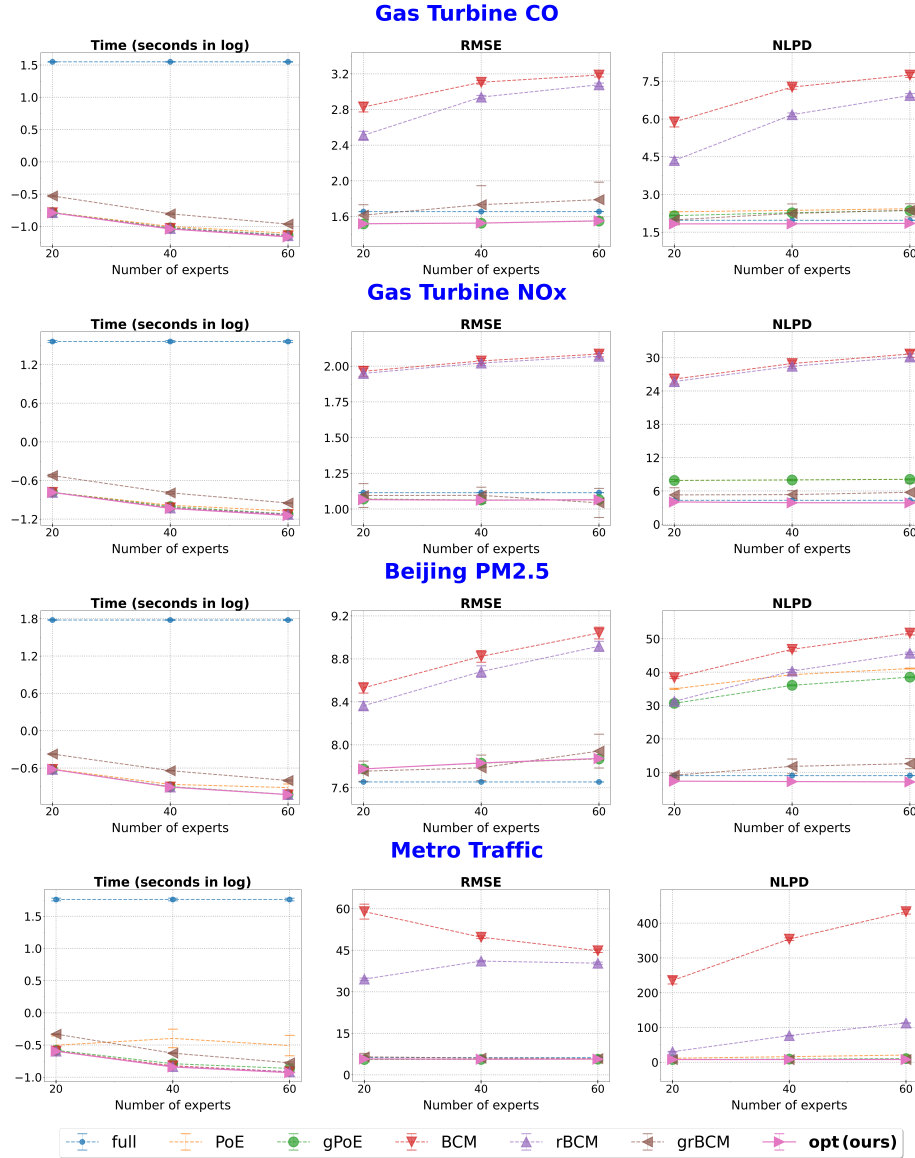


Figure 6: Comparison of aggregation models for SVGP on temporal extrapolation tasks. Models are trained on earlier years and tested on future years to evaluate performance under distribution shift.

Table 2: Results of aggregation models for SVGP on UCI datasets for temporal extrapolation tasks. Models are trained on earlier years and tested on future years. **Best** and **worst** performances are highlighted in yellow and red, respectively.

Data	M	Metric	SVGP	PoE	gPoE	BCM	rBCM	grBCM	opt (ours)
Gas Turbine CO	20	Time	35.405 ± 0.415	0.164 ± 0.002	0.164 ± 0.001	0.163 ± 0.001	0.164 ± 0.001	0.297 ± 0.001	0.163 ± 0.001
		RMSE	1.642 ± 0.053	1.518 ± 0.005	1.518 ± 0.005	2.828 ± 0.054	2.510 ± 0.045	1.615 ± 0.117	1.519 ± 0.005
		NLPD	1.955 ± 0.047	2.310 ± 0.009	2.157 ± 0.007	5.881 ± 0.195	4.350 ± 0.123	1.991 ± 0.199	1.830 ± 0.004
	40	Time	35.405 ± 0.415	0.100 ± 0.008	0.095 ± 0.005	0.094 ± 0.005	0.093 ± 0.005	0.157 ± 0.005	0.091 ± 0.005
		RMSE	1.656 ± 0.000	1.526 ± 0.002	1.525 ± 0.002	3.106 ± 0.020	2.939 ± 0.019	1.733 ± 0.214	1.527 ± 0.004
		NLPD	1.973 ± 0.000	2.366 ± 0.005	2.273 ± 0.006	7.269 ± 0.085	6.170 ± 0.071	2.244 ± 0.378	1.833 ± 0.004
	60	Time	35.405 ± 0.415	0.079 ± 0.007	0.074 ± 0.005	0.072 ± 0.002	0.072 ± 0.002	0.109 ± 0.001	0.069 ± 0.001
		RMSE	1.656 ± 0.000	1.550 ± 0.004	1.549 ± 0.005	3.187 ± 0.021	3.078 ± 0.020	1.789 ± 0.196	1.552 ± 0.005
		NLPD	1.973 ± 0.000	2.432 ± 0.010	2.360 ± 0.010	7.748 ± 0.094	6.935 ± 0.077	2.370 ± 0.261	1.849 ± 0.005
Gas Turbine NOx	20	Time	36.239 ± 1.322	0.164 ± 0.003	0.165 ± 0.003	0.164 ± 0.003	0.165 ± 0.003	0.299 ± 0.008	0.164 ± 0.003
		RMSE	1.065 ± 0.041	1.070 ± 0.012	1.070 ± 0.012	1.964 ± 0.035	1.949 ± 0.032	1.095 ± 0.083	1.066 ± 0.012
		NLPD	4.103 ± 0.446	7.900 ± 0.171	7.898 ± 0.176	26.145 ± 0.892	25.703 ± 0.802	5.297 ± 1.285	4.032 ± 0.100
	40	Time	36.239 ± 1.322	0.104 ± 0.007	0.099 ± 0.006	0.095 ± 0.004	0.094 ± 0.004	0.162 ± 0.008	0.092 ± 0.004
		RMSE	1.115 ± 0.000	1.063 ± 0.008	1.063 ± 0.008	2.036 ± 0.017	2.021 ± 0.016	1.096 ± 0.057	1.062 ± 0.013
		NLPD	4.332 ± 0.000	7.990 ± 0.126	7.987 ± 0.122	28.948 ± 0.476	28.460 ± 0.443	5.350 ± 0.713	3.890 ± 0.101
	60	Time	36.240 ± 1.322	0.084 ± 0.003	0.076 ± 0.005	0.075 ± 0.004	0.075 ± 0.003	0.112 ± 0.003	0.072 ± 0.002
		RMSE	1.115 ± 0.000	1.066 ± 0.007	1.066 ± 0.007	2.085 ± 0.020	2.069 ± 0.020	1.043 ± 0.102	1.065 ± 0.007
		NLPD	4.332 ± 0.000	8.104 ± 0.112	8.100 ± 0.111	30.656 ± 0.594	30.121 ± 0.565	5.759 ± 1.683	3.860 ± 0.053
Beijing PM2.5	20	Time	60.044 ± 1.202	0.242 ± 0.007	0.240 ± 0.007	0.240 ± 0.007	0.240 ± 0.007	0.422 ± 0.008	0.239 ± 0.007
		RMSE	7.780 ± 0.116	7.776 ± 0.016	7.775 ± 0.015	8.530 ± 0.048	8.363 ± 0.039	7.755 ± 0.094	7.775 ± 0.018
		NLPD	8.640 ± 0.652	35.010 ± 0.188	30.668 ± 0.299	38.362 ± 0.289	31.270 ± 0.280	9.147 ± 0.602	7.350 ± 0.100
	40	Time	60.044 ± 1.202	0.138 ± 0.008	0.127 ± 0.003	0.125 ± 0.002	0.125 ± 0.002	0.228 ± 0.002	0.124 ± 0.002
		RMSE	7.655 ± 0.000	7.830 ± 0.013	7.829 ± 0.013	8.823 ± 0.055	8.682 ± 0.054	7.786 ± 0.119	7.831 ± 0.010
		NLPD	9.020 ± 0.000	39.237 ± 0.137	36.061 ± 0.179	46.846 ± 0.554	40.320 ± 0.481	11.787 ± 2.199	7.232 ± 0.096
	60	Time	60.044 ± 1.202	0.123 ± 0.016	0.095 ± 0.003	0.094 ± 0.002	0.095 ± 0.003	0.159 ± 0.004	0.094 ± 0.002
		RMSE	7.655 ± 0.000	7.871 ± 0.012	7.869 ± 0.012	9.041 ± 0.055	8.917 ± 0.047	7.942 ± 0.157	7.873 ± 0.013
		NLPD	9.020 ± 0.000	41.091 ± 0.128	38.502 ± 0.151	51.722 ± 0.562	45.666 ± 0.351	12.596 ± 1.516	7.140 ± 0.095
Metro Traffic	20	Time	57.739 ± 2.806	0.317 ± 0.051	0.262 ± 0.010	0.255 ± 0.010	0.254 ± 0.009	0.467 ± 0.018	0.253 ± 0.010
		RMSE	6.065 ± 0.701	5.612 ± 0.099	5.534 ± 0.060	58.979 ± 2.695	34.593 ± 0.416	6.512 ± 1.272	5.741 ± 0.199
		NLPD	7.874 ± 0.083	11.481 ± 0.157	7.960 ± 0.023	235.124 ± 9.921	30.309 ± 1.069	7.942 ± 0.230	7.841 ± 0.026
	40	Time	57.739 ± 2.806	0.419 ± 0.118	0.162 ± 0.002	0.151 ± 0.004	0.146 ± 0.001	0.236 ± 0.003	0.144 ± 0.001
		RMSE	6.236 ± 0.000	5.587 ± 0.027	5.569 ± 0.020	49.724 ± 0.474	41.100 ± 0.278	6.050 ± 0.663	5.648 ± 0.067
		NLPD	7.893 ± 0.001	16.096 ± 0.074	9.088 ± 0.020	354.159 ± 3.765	76.711 ± 0.896	7.872 ± 0.145	7.843 ± 0.012
	60	Time	57.740 ± 2.806	0.330 ± 0.128	0.137 ± 0.004	0.122 ± 0.002	0.122 ± 0.002	0.167 ± 0.006	0.118 ± 0.001
		RMSE	6.236 ± 0.000	5.651 ± 0.023	5.638 ± 0.020	44.833 ± 0.618	40.345 ± 0.422	5.884 ± 0.406	5.692 ± 0.069
		NLPD	7.893 ± 0.001	20.677 ± 0.092	10.498 ± 0.038	433.313 ± 6.898	113.021 ± 0.620	7.829 ± 0.143	7.856 ± 0.012

6 Discussions

Conclusions In this work, we introduced an algorithm to enhance GP regressions with inducing points on sparse grids using the optimized combination technique (OptiCom). Building on this foundation, we proposed a novel aggregated prediction algorithm suitable for both distributed exact GP and SVGP. This method leverages predictions from local models and optimally combines them using weights derived from solving a linear system. Additionally, it inherently incorporates correlations between experts through the computation of optimal weights. The proposed methods have a computational complexity requiring $\mathcal{O}(M^3)$ additional time compared to PoE family and BCM family for M GP experts. However, this overhead is minimal in practice, as the number of experts M is typically small compared to the size of the local datasets. Through extensive experiments

and comparisons with state-of-the-art aggregation models, we demonstrated the competitiveness and stability of our proposed method. Our algorithm consistently provides stable and accurate predictions, offering a robust solution for distributed GP regression.

Practical considerations Beyond model design, practical deployment involves key trade-offs in choosing the number of experts and inducing points. The choice of the number of experts M involves a trade-off between efficiency and accuracy. Increasing M improves computational efficiency, as each expert handles a smaller subset of the data and can be trained in parallel. However, if M becomes too large, each expert receives too little data, degrading the quality of the local GP approximations. This effect is clearly illustrated in [Figure 4](#). In practice, we recommend selecting M based on empirical validation, such as cross-validation. A practical set of initial candidates can be defined as $M \in \{\lfloor \sqrt{n}/i \rfloor : i = 4, 5, 6\}$, where n is size of the global training data.

Similarly, the number of inducing points affects both accuracy and computational cost. More inducing points improve local approximations, and consequently lead to more accurate aggregated predictions, they also increase computational cost. In practice, selecting 5–10% of the local training data size as the number of inducing points provides a good balance.

Limitations While our method guarantees consistent predictive means in the limit, it does not ensure consistent predictive variances. Theoretically, variance consistency would require the aggregation weights to satisfy an additional ℓ_2 -norm condition, which we do not impose. As a result, variance estimates may be slightly less accurate compared to methods like grBCM, especially in uncertainty-sensitive applications.

Future directions A direction for future work is to extend our framework such that it also ensures variance consistency, potentially by modifying the weight optimization process or incorporating additional constraints. Furthermore, integrating adaptive selection of expert sizes and inducing points could further enhance the scalability and flexibility of the method in large-scale settings.

Acknowledgements

The authors acknowledge the generous support from the NSF grants DMS-2312173 and CNS-2328395. The experiments of this research were conducted on an A100 GPU provided by Texas A&M High Performance Research Computing.

Data availability statement

The data that support the findings of this study are openly available in (Asuncion and Newman, 2007) at <https://archive.ics.uci.edu/datasets>.

References

- Aronszajn, N. (1950). Theory of reproducing kernels. *Transactions of the American Mathematical Society*, 68(3):337–404.
- Asuncion, A. and Newman, D. (2007). UCI machine learning repository. <https://archive.ics.uci.edu/datasets>.
- Bishop, C. M. (1995). *Neural Networks for Pattern Recognition*. Oxford University Press.
- Boyd, S., Parikh, N., Chu, E., Peleato, B., and Eckstein, J. (2011). Distributed optimization and statistical learning via the alternating direction method of multipliers. *Foundations and Trends® in Machine Learning*, 3(1):1–122.
- Cao, Y. and Fleet, D. J. (2014). Generalized product of experts for automatic and principled fusion of Gaussian process predictions. *arXiv preprint arXiv:1410.7827*.
- Chen, H., Ding, L., and Tuo, R. (2022). Kernel packet: An exact and scalable algorithm for Gaussian process regression with Matérn correlations. *Journal of Machine Learning Research*, 23(127):1–32.
- Choi, T. (2005). *Posterior consistency in nonparametric regression problems under Gaussian process priors*. PhD thesis, Carnegie Mellon University.
- Dean, J., Corrado, G., Monga, R., Chen, K., Devin, M., Mao, M., Ranzato, M., Senior, A., Tucker, P., Yang, K., Le, Q. V., and Ng, A. Y. (2012). Large scale distributed deep networks. *Advances in Neural Information Processing Systems*, 25.
- Deisenroth, M. and Ng, J. W. (2015). Distributed Gaussian processes. In *International Conference on Machine Learning*, pages 1481–1490. PMLR.
- Deisenroth, M. P., Fox, D., and Rasmussen, C. E. (2013). Gaussian processes for data-efficient learning in robotics and control. *IEEE Transactions on Pattern Analysis and Machine Intelligence*, 37(2):408–423.
- Garcke, J. (2006). Regression with the optimised combination technique. In *Proceedings of the 23rd International Conference on Machine Learning*, pages 321–328.
- Garcke, J. (2013). Sparse grids in a nutshell. In *Sparse Grids and Applications*, pages 57–80. Springer.
- Griebel, M., Schneider, M., and Zenger, C. (1990). A combination technique for the solution of sparse grid problems. *Forschungsberichte, TU Munich*.
- Griewank, A. O. (1981). Generalized descent for global optimization. *Journal of Optimization Theory and Applications*, 34:11–39.

- Hartikainen, J. and Särkkä, S. (2010). Kalman filtering and smoothing solutions to temporal Gaussian process regression models. In *2010 IEEE International Workshop on Machine Learning for Signal Processing*, pages 379–384. IEEE.
- Hegland, M. (2002). Additive sparse grid fitting. In *Proceedings of the Fifth International Conference on Curves and Surfaces, Saint-Malo, France*, volume 2002.
- Hegland, M., Garcke, J., and Challis, V. (2007). The combination technique and some generalisations. *Linear Algebra and its Applications*, 420(2-3):249–275.
- Hinton, G. E. (2002). Training products of experts by minimizing contrastive divergence. *Neural Computation*, 14(8):1771–1800.
- Hogue, J. (2019). Metro Interstate Traffic Volume. UCI Machine Learning Repository. DOI: <https://doi.org/10.24432/C5X60B>.
- Katzfuss, M. and Guinness, J. (2021). A general framework for Vecchia approximations of Gaussian processes. *Statistical Science*, 36(1):124–141.
- Kaya, H., Tüfekci, P., and Uzun, E. (2019). Predicting CO and NOx emissions from gas turbines: Novel data and a benchmark PEMS. *Turkish Journal of Electrical Engineering and Computer Sciences*, 27(6):4783–4796.
- Kingma, D. P. and Ba, J. (2015). Adam: A method for stochastic optimization. In *International Conference on Learning Representations*.
- Kuss, M., Rasmussen, C. E., and Herbrich, R. (2005). Assessing Approximate Inference for Binary Gaussian Process Classification. *Journal of Machine Learning Research*, 6(10).
- Li, T., Sahu, A. K., Zaheer, M., Sanjabi, M., Talwalkar, A., and Smith, V. (2020). Federated optimization in heterogeneous networks. *Proceedings of Machine Learning and Systems*, 2:429–450.
- Liang, X., Zou, T., Guo, B., Li, S., Zhang, H., Zhang, S., Huang, H., and Chen, S. X. (2015). Assessing Beijing’s PM2.5 pollution: Severity, weather impact, APEC and winter heating. *Proceedings of the Royal Society A: Mathematical, Physical and Engineering Sciences*, 471(2182):20150257.
- Lin, J. A., Antorán, J., Padhy, S., Janz, D., Hernández-Lobato, J. M., and Terenin, A. (2023). Sampling from Gaussian process posteriors using stochastic gradient descent. *Advances in Neural Information Processing Systems*, 36:36886–36912.
- Lin, J. A., Padhy, S., Antorán, J., Tripp, A., Terenin, A., Szepesvári, C., Hernández-Lobato, J. M., and Janz, D. (2024). Stochastic gradient descent for Gaussian processes done right. In *International Conference on Learning Representations*.
- Liu, H., Cai, J., Wang, Y., and Ong, Y. S. (2018). Generalized robust Bayesian committee machine for large-scale Gaussian process regression. In *International Conference on Machine Learning*, pages 3131–3140. PMLR.
- Liutkus, A., Badeau, R., and Richard, G. (2011). Gaussian processes for underdetermined source separation. *IEEE Transactions on Signal Processing*, 59(7):3155–3167.
- McMahan, B., Moore, E., Ramage, D., Hampson, S., and y Arcas, B. A. (2017). Communication-efficient learning of deep networks from decentralized data. In *Artificial Intelligence and Statistics*, pages 1273–1282. PMLR.

O’Hagan, A. (1978). Curve fitting and optimal design for prediction. *Journal of the Royal Statistical Society: Series B (Methodological)*, 40(1):1–24.

Rasmussen, C. E. (2003). Gaussian processes in machine learning. In *Summer School on Machine Learning*, pages 63–71. Springer.

Rullière, D., Durrande, N., Bachoc, F., and Chevalier, C. (2018). Nested Kriging predictions for datasets with a large number of observations. *Statistics and Computing*, 28:849–867.

Smolyak, S. A. (1963). Quadrature and interpolation formulas for tensor products of certain classes of functions. In *Doklady Akademii Nauk*, volume 148, pages 1042–1045. Russian Academy of Sciences.

Titsias, M. (2009). Variational learning of inducing variables in sparse Gaussian processes. In *Artificial Intelligence and Statistics*, pages 567–574. PMLR.

Tresp, V. (2000). A Bayesian committee machine. *Neural Computation*, 12(11):2719–2741.

Wilson, A. and Nickisch, H. (2015). Kernel interpolation for scalable structured Gaussian processes (KISS-GP). In *International Conference on Machine Learning*, pages 1775–1784. PMLR.

A GP with OptiCom

In this section, we provide supporting figures for *optimized combination technique* (OptiCom) and detailed algorithms for GP with OptiCom in [Section A.1](#) and [Section A.2](#) respectively.

A.1 Figures

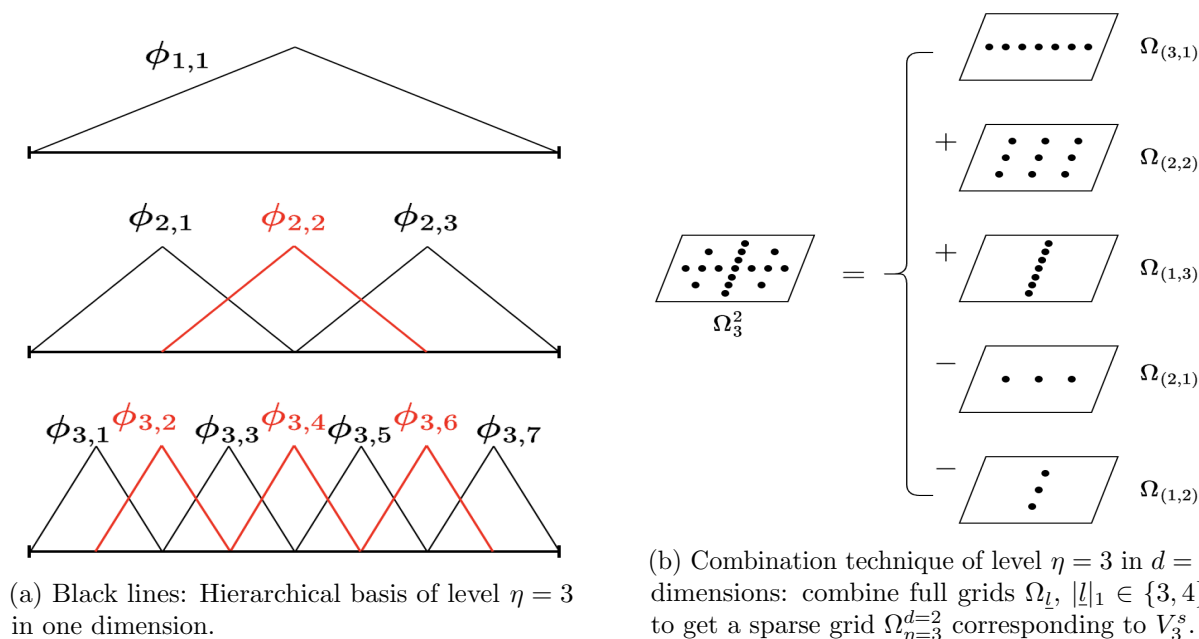


Figure 7: Basis functions and combination technique of level $\eta = 3$.

A.2 Algorithms

Algorithm 1 Optimal Coefficients for GP with OptiCom

- 1: **Input:** training inputs $\mathbf{X} = \{\mathbf{x}_i\}_{i=1}^n$, observations $\mathbf{y} = (y_1, \dots, y_n)^\top$, noise variance σ_ϵ^2 , a GP denoted by $\mathcal{GP}(\mu(\cdot), k(\cdot, \cdot))$, sparse grids Ω_η^d of level η and dimension d
- 2: **Output:** coefficients $\mathbf{c} = \{c_{\underline{l}^{(i)}}\}_{i=1}^b$, kernel weights $\{\alpha_{\underline{l}^{(i)}}\}_{i=1}^b$, Cholesky factors $\{\mathbf{L}_{\underline{l}^{(i)}}\}_{i=1}^b$, where $\{\underline{l}^{(i)}\}_{i=1}^b = \{\underline{l} : \eta \leq |\underline{l}|_1 \leq \eta + d - 1\}$
- 3: $\mathbf{A} := \text{zeros}(b, b)$
- 4: **for** $t = 0$ **to** $b - 1$ **do** # for loop over t and i can be parallelized
- 5: **for** $i = 1$ **to** $b - t$ **do** # loop over the diagonal with offset = t
- 6: $j := i + t$
- 7: $\mathbf{M} = [k(\Omega_{\underline{l}^{(i)}}, \Omega_{\underline{l}^{(j)}}) + \sigma_\epsilon^{-2} k(\Omega_{\underline{l}^{(i)}}, \mathbf{X}) k(\mathbf{X}, \Omega_{\underline{l}^{(j)}})]$
- 8: **if** $t = 0$ **then** # $i = j$, \mathbf{M} is symmetric and positive definite
- 9: $\mathbf{L}_{\underline{l}^{(i)}} := \text{chol}(\mathbf{M})$ s.t. $\mathbf{L}_{\underline{l}^{(i)}} \mathbf{L}_{\underline{l}^{(i)}}^\top = \mathbf{M}$
- 10: $\mathbf{R} := \mathbf{L}_{\underline{l}^{(i)}} \setminus [k(\Omega_{\underline{l}^{(i)}}, \mathbf{X}) \mathbf{y}]$
- 11: $\alpha_{\underline{l}^{(i)}} := \mathbf{L}_{\underline{l}^{(i)}}^\top \setminus \mathbf{R}$
- 12: **end if**
- 13: $\mathbf{A}[i, j] = \mathbf{A}[j, i] = \sigma_\epsilon^{-2} \alpha_{\underline{l}^{(i)}}^\top \mathbf{M} \alpha_{\underline{l}^{(j)}}$
- 14: **end for**
- 15: **end for**
- 16: $\mathbf{c} := \mathbf{A} \setminus \text{diag}(\mathbf{A})$
- 17: **return** \mathbf{c} , $\{\alpha_{\underline{l}^{(i)}}\}_{i=1}^b$, $\{\mathbf{L}_{\underline{l}^{(i)}}\}_{i=1}^b$

Algorithm 2 GP Posterior with OptiCom

- 1: **Input:** training inputs $\mathbf{X} = \{\mathbf{x}_i\}_{i=1}^n$, observations $\mathbf{y} = (y_1, \dots, y_n)^\top$, noise variance σ_ϵ^2 , test inputs $\mathbf{X}^* = \{\mathbf{x}_i^*\}_{i=1}^{n_t}$, a GP denoted by $\mathcal{GP}(\mu(\cdot), k(\cdot, \cdot))$, sparse grids Ω_η^d of level η and dimension d
- 2: **Output:** posterior mean $\hat{\mu}_\eta^c(\mathbf{X}^*)$ and posterior covariance $\hat{k}_\eta^c(\mathbf{X}^*, \mathbf{X}^*)$ in eq. (18)
- 3: $\mathbf{m} := \text{zeros}(n_t)$; $\mathbf{S} := \text{zeros}(n_t, n_t)$
- 4: get $\mathbf{c} = \{c_{\underline{l}^{(i)}}\}_{i=1}^b$, $\{\alpha_{\underline{l}^{(i)}}\}_{i=1}^b$, $\{\mathbf{L}_{\underline{l}^{(i)}}\}_{i=1}^b$ from Algorithm 1
- 5: **for** $i = 1$ **to** b **do** # for loop over i can be parallelized
- 6: $\mathbf{m} \leftarrow \mathbf{m} + c_{\underline{l}^{(i)}} k(\mathbf{X}^*, \Omega_{\underline{l}^{(i)}}) \alpha_{\underline{l}^{(i)}}$
- 7: $c_{\text{ct}} := (-1)^{\eta + d - 1 - |\underline{l}^{(i)}|_1} \binom{d-1}{|\underline{l}^{(i)}|_1 - \eta}$
- 8: $\mathbf{P} := k(\mathbf{X}^*, \Omega_{\underline{l}^{(i)}}) [k(\Omega_{\underline{l}^{(i)}}, \Omega_{\underline{l}^{(i)}})]^{-1} k(\Omega_{\underline{l}^{(i)}}, \mathbf{X}^*)$
- 9: $\mathbf{Q} := [k(\mathbf{X}^*, \Omega_{\underline{l}^{(i)}}) \mathbf{L}_{\underline{l}^{(i)}}^{-\top}] [\mathbf{L}_{\underline{l}^{(i)}}^{-1} k(\Omega_{\underline{l}^{(i)}}, \mathbf{X}^*)]$
- 10: $\mathbf{S} \leftarrow \mathbf{S} + c_{\text{ct}} [k(\mathbf{X}^*, \mathbf{X}^*) - \mathbf{P} + \mathbf{Q}]$
- 11: **end for**
- 12: $\hat{\mu}_\eta^c(\mathbf{X}^*) := \sigma_\epsilon^{-2} \mathbf{m}$
- 13: $\hat{k}_\eta^c(\mathbf{X}^*, \mathbf{X}^*) := \mathbf{S}$
- 14: **return** $\hat{\mu}_\eta^c(\mathbf{X}^*)$, $\hat{k}_\eta^c(\mathbf{X}^*, \mathbf{X}^*)$

B Distributed GP with optimal weights

In this section, we outline the algorithms of the proposed aggregation model for distributed SVGP and distributed exact GP in [Section B.1](#) and [Section B.2](#) respectively.

B.1 SVGP

Algorithm 3 Optimal Weights for Distributed SVGP

```

1: Input: local datasets  $\{\mathbf{X}_i, \mathbf{y}_i\}_{i=1}^M$ , noise variance  $\sigma_\epsilon^2$ , a GP denoted by  $\mathcal{GP}(\mu(\cdot), k(\cdot, \cdot))$ , inducing
   inputs  $\mathbf{Z} = \{\mathbf{z}_i\}_{i=1}^m$ 
2: Output: optimal weights  $\beta = \{\beta_i\}_{i=1}^M$ , kernel weights  $\{\alpha_i\}_{i=1}^M$ , Cholesky factors  $\{\mathbf{L}_i\}_{i=1}^M$ 
3:  $\mathbf{X}_c := \{\mathbf{x}_i^{(c)}\}_{i=1}^M$ ,  $\mathbf{x}_i^{(c)} \in \mathbf{X}_i$  is randomly selected
4:  $\mathbf{M}^{(c)} = [k(\mathbf{Z}, \mathbf{Z}) + \sigma_\epsilon^{-2}k(\mathbf{Z}, \mathbf{X}_c)k(\mathbf{X}_c, \mathbf{Z})]$ 
5:  $\mathbf{A} := \text{zeros}(M, M)$ 
6: for  $t = 0$  to  $M - 1$  do                                     # for loop over  $t$  and  $i$  can be parallelized
7:   for  $i = 1$  to  $M - t$  do                                       # loop over the diagonal with offset =  $t$ 
8:      $j := i + t$ 
9:     if  $t = 0$  then                                               #  $i = j$ 
10:       $\mathbf{M} = [k(\mathbf{Z}, \mathbf{Z}) + \sigma_\epsilon^{-2}k(\mathbf{Z}, \mathbf{X}_i)k(\mathbf{X}_i, \mathbf{Z})]$ 
11:       $\mathbf{L}_i := \text{chol}(\mathbf{M})$  s.t.  $\mathbf{L}_i\mathbf{L}_i^\top = \mathbf{M}$ 
12:       $\mathbf{R} := \mathbf{L}_i \setminus [k(\mathbf{Z}, \mathbf{X}_i)\mathbf{y}_i]$ 
13:       $\alpha_i := \mathbf{L}_i^\top \setminus \mathbf{R}$ 
14:    end if
15:     $\mathbf{A}[i, j] = \mathbf{A}[j, i] = \sigma_\epsilon^{-2}\alpha_i^\top \mathbf{M}^{(c)} \alpha_j$ 
16:  end for
17: end for
18:  $\beta := \mathbf{A} \setminus \text{diag}(\mathbf{A})$ 
19: return  $\beta$ ,  $\{\alpha_i\}_{i=1}^M$ ,  $\{\mathbf{L}_i\}_{i=1}^M$ 

```

Algorithm 4 Aggregated Prediction for Distributed SVGP

```

1: Input: local datasets  $\{\mathbf{X}_i, \mathbf{y}_i\}_{i=1}^M$ , noise variance  $\sigma_\epsilon^2$ , test inputs  $\mathbf{X}^* = \{\mathbf{x}_i^*\}_{i=1}^{n_t}$ , a GP denoted
   by  $\mathcal{GP}(\mu(\cdot), k(\cdot, \cdot))$ , inducing inputs  $\mathbf{Z} = \{\mathbf{z}_i\}_{i=1}^m$ 
2: Output: joint mean  $\mu_{\mathcal{A}}(\mathbf{X}^*)$  and joint variance  $\sigma_{\mathcal{A}}^2(\mathbf{X}^*)$  in eq. \(24\)
3: get  $\beta = (\beta_1, \dots, \beta_M)^\top$ ,  $\{\alpha_i\}_{i=1}^M$ ,  $\{\mathbf{L}_i\}_{i=1}^M$  from Algorithm 3
4:  $\mathbf{m} := \text{zeros}(n_t)$ ;  $\mathbf{s} := \text{zeros}(n_t)$ 
5: for  $i = 1$  to  $M$  do                                             # for loop over  $i$  can be parallelized
6:    $\mathbf{m} \leftarrow \mathbf{m} + \beta_i k(\mathbf{X}^*, \mathbf{Z}) \alpha_i$ 
7:    $\mathbf{R} := \mathbf{L}_i \setminus K(\mathbf{Z}, \mathbf{X}^*)$ 
8:    $\mathbf{s} \leftarrow \mathbf{s} + \beta_i^2 \mathbf{R}^\top \mathbf{R}$ 
9: end for
10:  $\mu_{\mathcal{A}}(\mathbf{X}^*) := \sigma_\epsilon^{-2} \mathbf{m}$ 
11:  $\sigma_{\mathcal{A}}^2(\mathbf{X}^*) := \mathbf{s}$ 
12: return  $\mu_{\mathcal{A}}(\mathbf{X}^*)$ ,  $\sigma_{\mathcal{A}}^2(\mathbf{X}^*)$ 

```

B.2 Exact GP

Algorithm 5 Optimal Weights for Distributed Exact GP

```

1: Input: local datasets  $\{\mathbf{X}_i, \mathbf{y}_i\}_{i=1}^M$ , noise variance  $\sigma_\epsilon^2$ , a GP denoted by  $\mathcal{GP}(\mu(\cdot), k(\cdot, \cdot))$ 
2: Output: optimal weights  $\beta = \{\beta_i\}_{i=1}^M$ , kernel weights  $\{\alpha_i\}_{i=1}^M$ , Cholesky factors  $\{\mathbf{L}_i\}_{i=1}^M$ 
3:  $\mathbf{X}_c := \{\mathbf{x}_i^{(c)}\}_{i=1}^M$ ,  $\mathbf{x}_i^{(c)} \in \mathbf{X}_i$  is randomly selected
4:  $\mathbf{A} := \text{zeros}(M, M)$ 
5: for  $t = 0$  to  $M - 1$  do                                     # for loop over  $t$  and  $i$  can be parallelized
6:   for  $i = 1$  to  $M - t$  do                                       # loop over the diagonal with offset =  $t$ 
7:      $j := i + t$ 
8:      $\mathbf{M}^{(c)} = [k(\mathbf{X}_i, \mathbf{X}_j) + k(\mathbf{X}_i, \mathbf{X}_c)k(\mathbf{X}_c, \mathbf{X}_i)]$ 
9:     if  $t = 0$  then                                               #  $i = j$ 
10:       $\mathbf{L}_i := \text{chol}(\tilde{\mathbf{K}}_{\mathbf{f}_i \mathbf{f}_i})$  s.t.  $\mathbf{L}_i \mathbf{L}_i^\top = \tilde{\mathbf{K}}_{\mathbf{f}_i \mathbf{f}_i} = k(\mathbf{X}_i, \mathbf{X}_i) + \sigma_\epsilon^2 \mathbf{I}_{n_i}$ 
11:       $\mathbf{R} := \mathbf{L}_i \setminus \mathbf{y}_i$ 
12:       $\alpha_i := \mathbf{L}_i^\top \setminus \mathbf{R}$ 
13:    end if
14:     $\mathbf{A}[i, j] = \mathbf{A}[j, i] = \alpha_i^\top \mathbf{M}^{(c)} \alpha_j$ 
15:  end for
16: end for
17:  $\beta := \mathbf{A} \setminus \text{diag}(\mathbf{A})$ 
18: return  $\beta$ ,  $\{\alpha_i\}_{i=1}^M$ ,  $\{\mathbf{L}_i\}_{i=1}^M$ 

```

Algorithm 6 Aggregated Prediction for Distributed Exact GP

```

1: Input: local datasets  $\{\mathbf{X}_i, \mathbf{y}_i\}_{i=1}^M$ , noise variance  $\sigma_\epsilon^2$ , test inputs  $\mathbf{X}^* = \{\mathbf{x}_i^*\}_{i=1}^{n_t}$ , a GP denoted
   by  $\mathcal{GP}(\mu(\cdot), k(\cdot, \cdot))$ 
2: Output: joint mean  $\mu_{\mathcal{A}}(\mathbf{X}^*)$  and joint variance  $\sigma_{\mathcal{A}}^2(\mathbf{X}^*)$  in eq. (26)
3: get  $\beta = (\beta_1, \dots, \beta_M)^\top$ ,  $\{\alpha_i\}_{i=1}^M$ ,  $\{\mathbf{L}_i\}_{i=1}^M$  from Algorithm 5
4:  $\mathbf{m} := \text{zeros}(n_t)$ ;  $\mathbf{s} := \text{zeros}(n_t)$ 
5: for  $i = 1$  to  $M$  do                                             # for loop over  $i$  can be parallelized
6:    $\mathbf{m} \leftarrow \mathbf{m} + \beta_i k(\mathbf{X}^*, \mathbf{X}_i) \alpha_i$ 
7:    $\mathbf{R} := \mathbf{L}_i \setminus k(\mathbf{X}_i, \mathbf{X}^*)$ 
8:    $\mathbf{s} \leftarrow \mathbf{s} + \beta_i^2 \mathbf{R}^\top \mathbf{R}$ 
9: end for
10:  $\mu_{\mathcal{A}}(\mathbf{X}^*) := \mathbf{m}$ 
11:  $\sigma_{\mathcal{A}}^2(\mathbf{X}^*) := \mathbf{s}$ 
12: return  $\mu_{\mathcal{A}}(\mathbf{X}^*)$ ,  $\sigma_{\mathcal{A}}^2(\mathbf{X}^*)$ 

```

C Experiment

In this section, we provide the supporting boxplots for the distributed training on synthetic data and tables for the aggregation models on UCI datasets in Section C.1.

C.1 Boxplots of the hyperparameter estimates



Figure 8: Boxplots of the optimized hyperparameter estimates on the $n = 10^4$ dataset.